Journal of
Medicinal Chemistry

Article

Structure-Activity Relationship Study Enables the Discovery of a Novel Berberine Analogue as RXR# Activator to Inhibit Colon Cancer

Beibei Xu, Xunjin Jiang, Jing Xiong, Jun Lan, Yuan Tian, LINHAI ZHONG, Xinquan Wang, Ning Xu, Hanwei Cao, Wenqing Zhang, Hao Zhang, Xiaoting Hong, Yan-yan Zhan, Yandong Zhang, and Tianhui Hu

J. Med. Chem., **Just Accepted Manuscript** • DOI: 10.1021/acs.jmedchem.0c00088 • Publication Date (Web): 11 May 2020

Just Accepted

is published by the American Chemical Society. 1155 Sixteenth Street N.W., Washington, DC 20036

Structure-Activity Relationship Study Enables the Discovery of a Novel Berberine Analogue as RXRα Activator to Inhibit Colon Cancer

Beibei Xu,[†,#] Xunjin Jiang,[‡,#] Jing Xiong,[†] Jun Lan,[§] Yuan Tian,[†] Linhai Zhong,[†] Xinquan Wang,[§] Ning Xu,[§] Hanwei Cao,[†] Wenqing Zhang,[†] Hao Zhang,[∥] Xiaoting Hong,[†] Yan-yan Zhan,[,†] Yandong Zhang[*,‡] and Tianhui Hu[*,†]*

[†]Cancer Research Center, School of Medicine, Xiamen University, Xiamen, 361005, China

[‡]Department of Chemistry and Key Laboratory of Chemical Biology of Fujian Province, iChEM, College of Chemistry and Chemical Engineering, Xiamen University, Xiamen, Fujian 361005, China

[§]Department of Biological Sciences, Tsinghua University, Beijing 100084, China;

[∥]Department of pathology, Jinan University Medical College, Guangzhou, 510632, China

[#]These authors contributed equally.

[*]To whom all correspondence should be addressed. Emails: yyzhan@xmu.edu.cn, ydzhang@xmu.edu.cn, thu@xmu.edu.cn

KEY WORDS: berberine analogue; RXRα activator; structure-activity analysis; B-12; colon cancer

ABSTRACT : We reported recently that berberine, a traditional oriental medicine to treat gastroenteritis, binds and activates Retinoid X receptor α (RXRα) to suppress the growth of colon cancer cells. Here, we extended our studies based on the binding mode of berberine with RXRα by design, synthesis and biological evaluation of a focused library of 15 novel berberine analogues. Among them, 3,9-dimethoxy-5,6-dihydroisoquinolino[3,2-a]isoquinolin-7-ium chloride (**B-12**) was identified as the optimal RXRα activator. More efficiently than berberine, **B-12** bound and altered the conformation of RXRα/LBD, thereby suppressing Wnt/β-catenin pathway and colon cancer cell growth via RXRα mediation. In addition, **B-12** not only preserved berberine's tumor selectivity but also greatly improved its bioavailability. Remarkably, in mice, **B-12** did not show obvious side effects including hypertriglyceridemia as other RXRα agonists, or induce hepatorenal toxicity. Together, our study describes an approach for the rational design of berberine-derived RXRα activators as novel effective antineoplastic agents for colon cancer.

■ INTRODUCTION

Colon cancer is the third most common malignancy and the fourth leading cause of cancer-related deaths worldwide. It is initiated in the epithelial cells lining the colon or rectum and frequently results from Wnt/β-catenin signaling pathway overactivation that is driven by mutations in pathway components, such as adenomatous polyposis coli (APC) and β-catenin.[1] In the past two decades, the survival rate has increased significantly profiting from multiple new therapeutic methods. However, the 5-year disease-specific overall survival rate is still lower than 60% due to tumor recurrences and drug resistances.[2, 3] New agents targeting important molecules in colon cancer development, with potent antitumor efficacy and low toxicity, is still urgently needed.

Retinoid X receptor α (RXRα), a unique member of the nuclear receptor superfamily, participates in a wide range of cellular processes under physiological and pathophysiological conditions through modulating gene expression in a ligand-dependent manner. The abnormal expression or post-translational modification of RXRα is closely related to the development of several types of cancers, such as colon cancer.[4-6] Hyperphosphorylation of RXRα, resulting in its transactivation inhibition, was detected in a series of human colon cancer cell lines and primary human colon cancer tissues.[7] RXRα expression was also downregulated in *APC* mutant mice.[8] Proteomics analyses demonstrated that more than 70% of the significantly down-regulated proteins are associated with abnormal RXRα signaling pathway in colon cancer tissues.[9] Additionally, extensive crosstalk between RXRα and Wnt/β-catenin signaling pathway was also observed in colon cancer.[10, 11] Suppression of RXRα and aberrant β-catenin expression significantly associate with progression of colon cancer.[12, 13] RXRα agonists increased β-catenin and RXRα protein interaction, leading to the degradation of β-catenin and the inhibition of cell growth in colon cancer.[14, 15] Therefore, RXRα is considered to be an important target for colon cancer treatment. Identifying and optimizing molecules that bind to its canonical ligand-binding pocket (LBP) has long been the focus of drug discovery efforts targeting RXRα, and a large pool of such RXRα ligands have been reported, such as 9-*cis*-retinoid acid (9-*cis*-RA), targretin (LGD1069) and sulindac.[16, 17] However, there are key limitations of treatment with these ligands including unwanted side effects such as hypertriglyceridemia, mucosal toxicity, hypercalcemia, and hepatomegaly.[4, 16-18] The current challenge is to discover selective RXRα modulators with desired pharmacological activities and minimal undesired side effects.[4, 16, 17]

Berberine (Figure 1a), an isoquinoline alkaloid isolated from several Chinese herbs such as *Coptis chinensis*, is a nonprescription medicine traditionally used to treat gastroenteritis. In recent

years, pharmacological and clinical studies have displayed a broad range of benefits from berberine treatment, including antidiabetic, antihyperlipidemic, and antitumor effects.[19-22] In several cancer models, berberine has been proven to reduce cell proliferation, induce cell apoptosis and inhibit tumor angiogenesis and metastasis, which makes berberine a promising drug for cancer therapy.[23, 24] Notably, berberine is a radiosensitizer of tumor cells but not normal, untransformed cells, and also displays high selectivity for colon cancer cells relative to normal colon epithelial cells.[25] Our recent study demonstrated that berberine acted as a novel RXRα activator to suppress β-catenin signaling and cell growth in colon cancer through directly binding to a unique site (Site X) on the ligand-binding domain (LBD) of RXRα, which is likely the main reason for the tumor selectivity of berberine and thus provided new strategies for the design of new RXRα-based antitumor agents.[26] However, some limitations of berberine, including poor solubility, low bioavailability, and moderate tumor-suppressing activity,[27, 28] restrict its clinical application to treat colon cancer. Structural modification of berberine would be an effective way to solve this dilemma. Some modifications of berberine have been carried out trying to improve its bioactivity and bioavailability in antimicrobial, antidiabetic, antihyperlipidemic and antitumor effects. Modification at C8 and C13 greatly increased the antimicrobial activity of berberine, which is closely related to the substituent chain length.[29-31] Most of the berberine derivatives with halogen and heteroaromatics on C8, C9 position displayed stronger hypoglycemic ability than berberine.[32, 33] Structure-activity studies on the antitumor effect of berberine mainly focused on the C8, C9, and C13 positions; for example, 13-alkyl derivatives of berberine showed higher antitumor activities than berberine, and a moderate alkyl chain length was beneficial for its antitumor activity.[34-36] However, almost all these modifications are randomly made and effect-oriented, lacking a structural basis for the mechanism of berberine's effects. Most of these derivatives, by inserting

either a long aliphatic chain or a heterocyclic ring, may have significant effects but lose the biosafety of berberine since the structures were changed too much. Moreover, these derivatives were mostly accessed by modification of natural berberine, thus significantly restricting the structural diversity necessary for structure-activity relationship (SAR) studies.

Our previous studies identified RXRα as an intracellular target of berberine to suppress colon cancer growth and disclosed a unique binding mode of berberine with RXRα,[26] which provides an ideal theoretical base for SAR design of new anti-tumor berberine analogues. In the present study, based on our previous findings, we designed and prepared 15 berberine analogues (nine of them are new compounds) in a total synthesis manner with modifications on the C2/3/9/10/11/12 positions of berberine, in an attempt to find a molecule possessing similar tumor-selectivity to that of berberine but with enhanced antitumor activity and bioavailability.

■ RESULTS

Design and synthesis of berberine analogues targeting RXRα

We described recently how berberine (Figure 1a) acts as an RXRα activator through direct binding to the Site X (non-classical ligand-binding pocket) in the ligand-binding domain (LBD) of RXRα to activate its transactivating function and its regulation on Wnt/β-catenin signaling to inhibit colon cancer growth; the C2, C3 groups on the head of berberine form H-bonds with the Arg371 residue of RXRα, and the C9, C10 methoxy groups on the tail region of berberine form Van Der Waals contacts with RXRα (Figure 1b).[26] To obtain more efficient RXRα activator and overcome aforementioned drawbacks residing in berberine as a promising antineoplastic agent, we designed 15 berberine analogues with modifications on C2, 3, 9, 10, 11 and 12 positions based on

the mode of berberine binding to RXRα. The structures of these analogues were shown in Table 1.

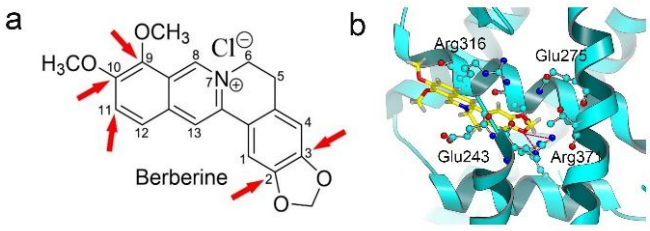

Figure 1. Chemical structure of berberine (a) and the binding site in RXRα-LBD (b)

(**a**) Chemical structure of berberine. Red arrows indicated the sites to be remodeled. (**b**) Detailed view of the interaction between berberine (yellow) and RXRα/LBD (cyan) (PDB:3FUG) in Site X. Key residues involved in berberine binding were shown in sticks; potential hydrogen-bonding interaction between berberine and RXRα-LBD residues Arg371 was shown as dashed red line.

The analogues of berberine were prepared according to Donohoe's protocol[37] and a general synthetic sequence was illustrated in Scheme 1. The acetophenone **3** could be synthesized from the substituted phenylacetic acids through reduction followed by the protection of the resulting alcohol as a pivalate and a regioselective Friedel-Crafts acylation reaction with Ac_2O and $ZnCl_2$. Aryl bromide **6** was prepared from the corresponding *o*-bromobenzaldehyde through acetal protection. Then in the presence of $[(Amphos)_2PdCl_2]$ and Cs_2CO_3, the cross-coupling between acetophenone **3** and aryl bromide **6** delivered **7**. Finally, the desired berberine analogue was formed by heating the mixture of compound **7** and NH_4Cl in $EtOH/H_2O$. Through this reaction sequence, 15 berberine analogues, named **B-1** to **B-15**, were synthesized smoothly (Figure 2b). Among them,

B-2 (pseudocoptisine),[38] **B-4** (pseudoberberine),[39] **B-5** (pseudopalmatine),[40] and **B-11** (palmatine)[41] are natural products and **B-1**[42] and **B-9**[42] are known berberine analogues. The structure and purity (above 95% pure) of all berberine analogues were confirmed by qNMR analysis techniques. Berberine and its 15 analogues were screened by PAINS-remover (http://www.cbligand.org/PAINS) to filter out potential false-positive molecules and all these analogues were proved to be PAIN-less.

Scheme 1.Synthesis of berberine analogues

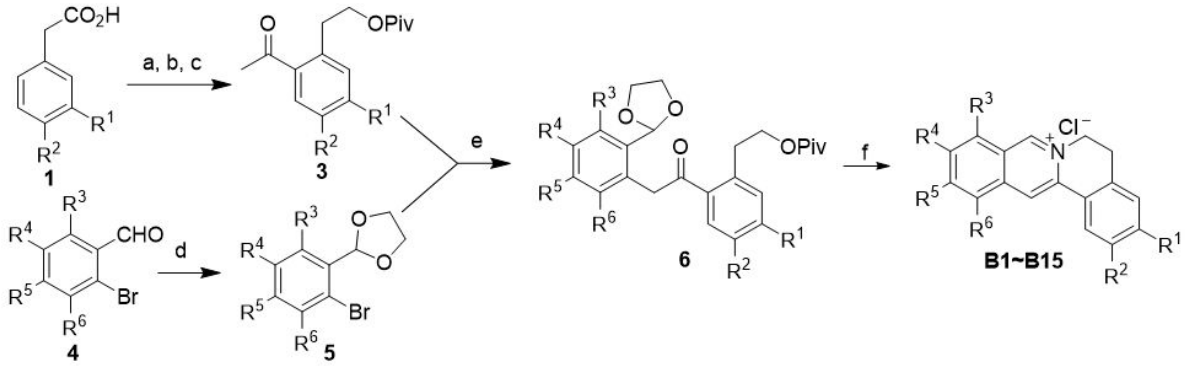

Reagents and conditions: (a) $BH_3 \cdot HF$ (2.0 equiv), THF, 0 °C→rt; (b) PivCl (2.0 equiv), pyridine (2.0 equiv), CH_2Cl_2, 0 °C→rt; (c) $ZnCl_2$ (5.0 equiv), Ac_2O, 0 °C→rt; (d) ethylene glycol (5.0 equiv), PTSA (0.1 equiv), $HC(OEt)_3$ (3.0 equiv), toluene, 90 °C; (e) $[(Amphos)_2PdCl_2]$ (5 mol%), Cs_2CO_3 (2.5 equiv), THF, 90 °C; (f) NH_4Cl, $EtOH/H_2O$ (3:1), 90 °C then 110 °C.

Table 1. Structures of the berberine analogues

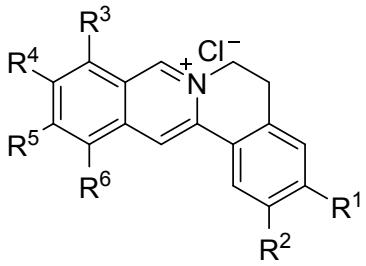

Compound	R1	R2	R3	R4	R5	R6
B-1	OCH_2O		H	H	H	H
B-2	OCH_2O		H	OCH_2O		H
B-3	OCH_3	H	H	OCH_3	OCH3	H
B-4	OCH_2O		H	OCH_3	OCH_3	H
B-5	OCH_3	OCH_3	H	OCH_3	OCH_3	H
B-6	OCH_3	OCH_3	H	H	H	H
B-7	OCH_3	H	H	H	H	H
B-8	OCH_3	H	H	OCH_2O		H
B-9	OCH_2O		H	OCH_3	H	H
B-10	OCH_3	H	OCH_3	OCH_3	H	H
B-11	OCH_3	OCH_3	OCH_3	OCH_3	H	H
B-12	OCH_3	H	OCH_3	H	H	H
B-13	OCH_3	OCH_3	OCH_3	H	H	H
B-14	OCH_3	OCH_3	H	H	H	OCH_3
B-15	OCH_2O		H	H	H	OCH_3

*Structure-activity analyses identified **B-12** as the most effective RXRα activator among these berberine analogues*

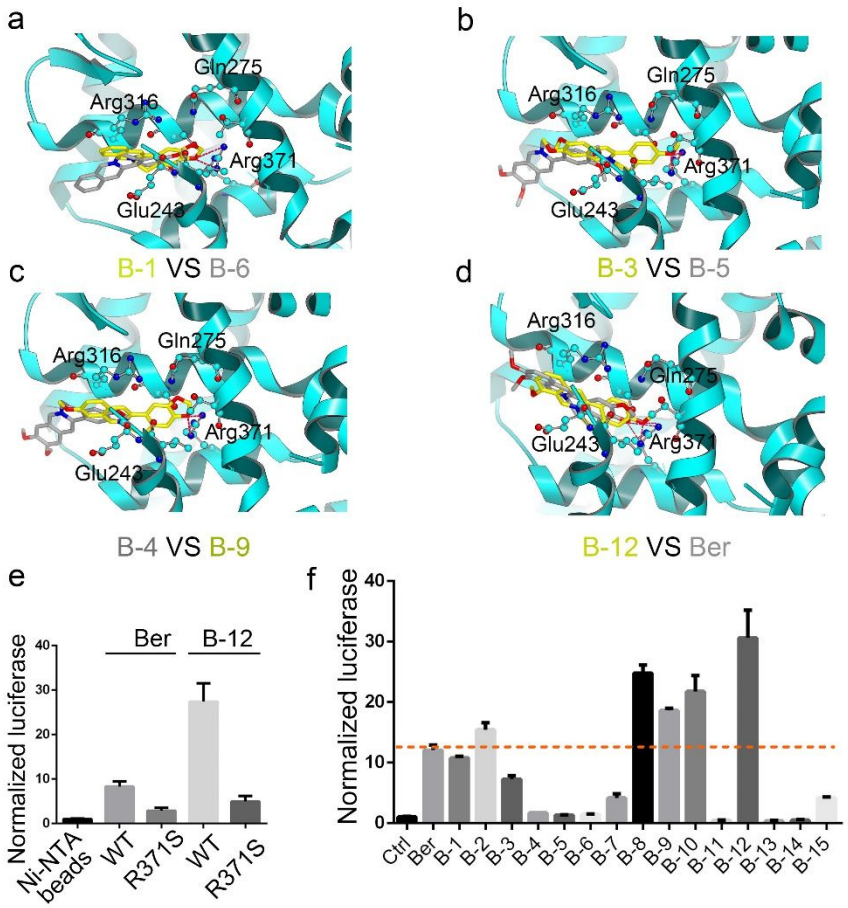

Figure 2. Structure-activity analyses identified **B-12** as the most effective RXRα activator among these berberine analogues. (**a-d**) Close-up view of the berberine analogues binding to RXRα-LBP (PDB code 3FUG). Compounds **B-1**, **B-3**, **B-9**, and **B-12** were shown in yellow; and compounds **B-4**, **B-5**, **B-6** and **Berberine (Ber)** were indicated in gray. Key residues involved in RXRα binding were shown in sticks. Potential hydrogen-bonding interaction between berberine analogues and RXRα/LBD Arg371 was shown as a dashed red line. (**e**) KM12C cells were co-transfected with pG5luc plasmid and pBIND-RXRα-LBD or its mutants. Twenty hours after

transfection, cells were treated with 50 μM berberine or **B-12**; then the activities of the reporter gene were determined by luciferase assays and the basal level was normalized to 1. (**f**) KM12C cells co-transfected with pBIND-RXRα/LBD and pG5luc were treated with berberine or its analogues at 50 μM for 15 h.

With these compounds in hand, we carried out SAR studies by evaluating binding affinity to RXRα through molecular docking studies and further by biological tests (Figure 2 and Table 2). Firstly, the docking calculations suggested that the compounds with 2,3-methylenedioxy group have much better binding conformation than that with 2,3-dimethoxy group. As shown in Figure 2a, the C3-oxygen of **B-1** formed two H-bonds with the backbone of Arg371 in RXRα/LBD, while **B-6** could not form any effective interactions with the surrounding amino acid residues. We next found that the single C3 methoxy group of **B-3** is also beneficial for the compound to bind RXRα-LBD, while the C2 methoxy group in compound **B-5** seemed to hamper the compound to enter the binding-pocket and form H-bond with Arg371 of RXRα by comparing **B3** and **B5** (Figure 2b), which might result from the larger steric hindrance induced by the coexistence of C2 and C3 methoxy groups. Next, we investigated the roles of functional groups present on the C9/10/11/12 positions (the tail) of berberine core when the compounds have the same head structure. By comparing **B-4** with **B-9**, we found 10,11-dimethoxy groups seemed to impede the binding of the compounds with RXRα/LBD, because even though **B-4** has a methylenedioxy group at C2-C3 positions, which is more favorable for binding to RXR protein, it is still almost outside the pocket (Figure 2c). Similar docking results mentioned above were obtained when comparing **B-14** and **B-15**, **B-12** and **B-13**, **B-2** and **B-4**, respectively (Figure S1a-c). It is worth noting, when the heads of compounds bear C3 single methoxy or 2,3-methylenedioxy groups, some analogues with

substituents on the C9/10/11 positions of berberine, except the analogues with bismethoxy groups on C10 and C11 (**B-3** and **B-4**), could well match the binding-pocket and form H-bonds with Arg371, such as **B-2**, **B-8**, **B-9**, **B-10** and **B-12** (Figure S1d).

For further verification, we ranked the binding potential of berberine analogues with RXRα/LBD through molecular docking by four indexes, including shape matching, H-bond energy, protein solvation, and small molecule solvation. As shown in Table 1, the five top-scoring compounds are **B-12**, **B-8**, **B-9**, **B-10** and **B-2**, which is consistent with the above conformational analysis. Next, the physiological consequences of the interactions between these compounds and RXRα/LBD were validated by their abilities to transactivate RXRα (Figure 2f), as well as to inhibit colon cancer cell growth, which were illustrated as IC_{50} in Table 2. The dose-response curves of representative compounds (**Ber**, **B-8**, **B-9**, **B-10**, **B-12**), along with 9-*cis*-RA as positive control, were shown in Figure S1e. The above results illustrated that compounds with higher binding potential to RXRα as indicated in molecular docking analysis indeed had a stronger ability to stimulate the transactivation activities of RXRα/LBD and inhibit the growth of colon cancer cells, such as **B-8**, **B-9**, **B-10** and **B-12**; reversely, those showing poor binding potential exhibited little effect on the RXRα-LBD transactivation activity and inhibition of colon cancer cell proliferation, including **B-4**, **B-5**, **B-6**, **B-7**, **B-13**, and **B-14**. Among all these compounds, **B-12**, as expected, exhibited the strongest transcriptional activation ability to RXRα and the greatest inhibitory effect on colon cancer cell growth (Figure 2f and Table 2). **B-12** has the lowest IC_{50} value to KM12C cell growth (31.10 μM), which was much smaller than that of berberine (76.34 μM). Based on these results, we further explored the binding conformation of compound **B-12**, and the results indicated that compound **B-12** manifested a better binding conformation with RXRα/LBD (Figure 2d), and its H-bond lengths with Arg371 of RXRα (3.0 Å, 3.11 Å) was far shorter than that of

berberine (3.9 Å, 3.2 Å). Subsequent mutation analysis confirmed that Arg371 is essential for the binding of RXRα/LBD with both **B-12** and berberine (Figure 2e). We further confirmed the superiority of **B-12** to berberine on cancer cell growth and RXRα-dependent transactivation in another two colon cancer cell lines HCT116 and SW620. Results showed that **B-12** exhibited excellent IC_{50} values in the growth inhibition of HCT116 and SW620 cells (27.17 μM and 36.19 μM, respectively), which were less than one-third of that of berberine (83.09 μM and 126.20 μM, respectively) (Figure S2a). **B-12** also acted much better than berberine to suppress colon cancer cell growth indicated by EdU (5-Ethynyl-2'-deoxyuridine) assay and PCNA (proliferating cell nuclear antigen, a cell proliferation marker) expression level (Figure S2b-c), and to enhance the transactivation activity of endogenous RXRα on RXR DNA response element (RXRE) in KM12C, HCT116 and SW620 cells (Figure S2d).

Table 2. Berberine analogues' molecular docking conformational analysis score sheet and their inhibitory effects (IC_{50}) on KM12C cell proliferation

Compound	Total Score	Hydrogen Bond	Shape	Ligand Desolvation	Protein Desolvation	IC_{50} (μM)
B-1	5.42	-0.92	-11.68	1.03	6.15	79.70
B-2	5.60	-0.94	-13.55	1.37	7.39	57.18
B-3	5.38	-0.98	-12.35	0.65	7.30	83.50
B-4	4.84	-0.96	-8.45	1.28	6.68	467.00
B-5	4.64	-0.21	-10.67	0.76	6.13	**>** 600
B-6	4.00	-0.49	-10.66	1.18	5.96	**>** 600
B-7	5.39	-0.83	-11.47	0.60	6.30	128.80
B-8	5.90	-0.69	-13.36	1.17	6.97	46.37
B-9	5.81	-0.81	-12.52	0.71	6.82	52.69

B-10	5.77	-0.98	-13.39	1.04	7.35	37.88
B-11	3.78	-0.89	7.83	1.31	-11.58	393.00
B-12	6.01	-0.95	-13.39	0.90	7.09	31.10
B-13	3.59	-0.11	-10.90	1.06	6.35	166.00
B-14	3.94	-0.47	-9.10	0.97	3.97	270.00
B-15	4.88	-0.81	-11.56	1.35	6.14	118.40
Ber	5.53	-0.90	-13.24	1.37	7.39	76.34

*Evaluation of **B-12** binding ability with RXRα*

Molecular docking and bio-activity analysis above picked **B-12** out as the most distinguished activator of RXRα among these 15 newly-synthesized berberine analogues (Figure 2). Several biophysicochemical methods were then employed to examine the binding ability of **B-12** with RXRα. Firstly, we determined the physical interaction between **B-12** and RXRα/LBD by saturation transfer difference (STD)-NMR spectroscopy. As shown in Figure 3a, the ^{1}H NMR spectra with and without **B-12** were obtained, and most signals were observed in STD-NMR spectra showing that RXRα/LBD protein interacts with **B-12**. We then used fluorescence quenching analysis to evaluate the binding affinity of **B-12** to RXRα/LBD. His-RXRα/LBD displayed maximal fluorescence at 332 nm (Figure 3b, left panel). When the concentration of **B-12** or berberine was increased from 0 to 30 μM, the fluorescence intensity of RXRα/LBD gradually decreased, without a significant shift of the maximum fluorescence emission wavelength (Figure 3b, left panel). Plotting of the data yielded titration curves (Figure 3b, right panel), from which the apparent dissociation constants (K_d) value was calculated as 1.89×10^{-5} M and 2.48×10^{-5} M for **B-12** and berberine binding to RXRα/LBD proteins, respectively. Finally, CD spectroscopic assay was performed to test whether **B-12** could induce a change in the conformation of His-RXRα/LBD. The far-UV CD spectrum of His-RXRα/LBD exhibited two negative peaks at 208 nm and 222 nm

and a positive peak at 192 nm, suggesting the presence of α-helical structure (Figure 3c). Upon **B-12** binding, this conformation of His-RXRα/LBD was significantly changed, to a greater extent than that induced by berberine (Figure 3c). These results indicated that **B-12** directly interacted with RXRα/LBD and altered its conformation, and the binding affinity of **B-12** with RXRα/LBD was stronger than that of berberine.

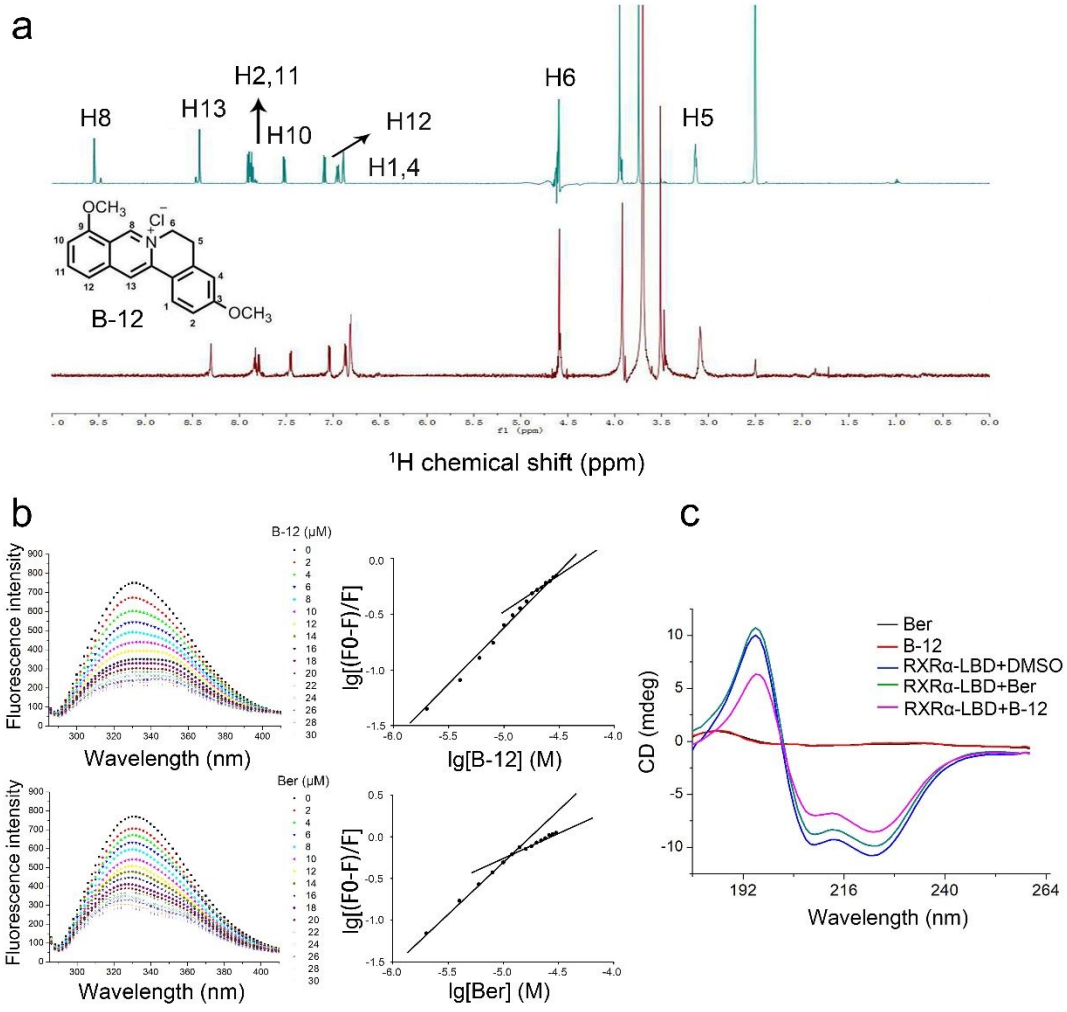

Figure 3. B-12 directly bound to RXRα/LBD. (**a**) STD spectrum of **B-12** and RXRα/LBD. The green spectra represented the ^{1}H NMR spectra of **B-12** alone. The red spectra represented the ^{1}H NMR spectra of **B-12** and RXRα incubated together. (**b**) Fluorescence quenching spectra (left)

and Stern-Volmer plot (right) for RXRα/LBD-berberine/**B-12** interaction. (**c**) CD spectroscopic analysis of the binding of berberine and **B-12** (5 μM) to RXRα/LBD (1 μM) with consequent conformational changes.

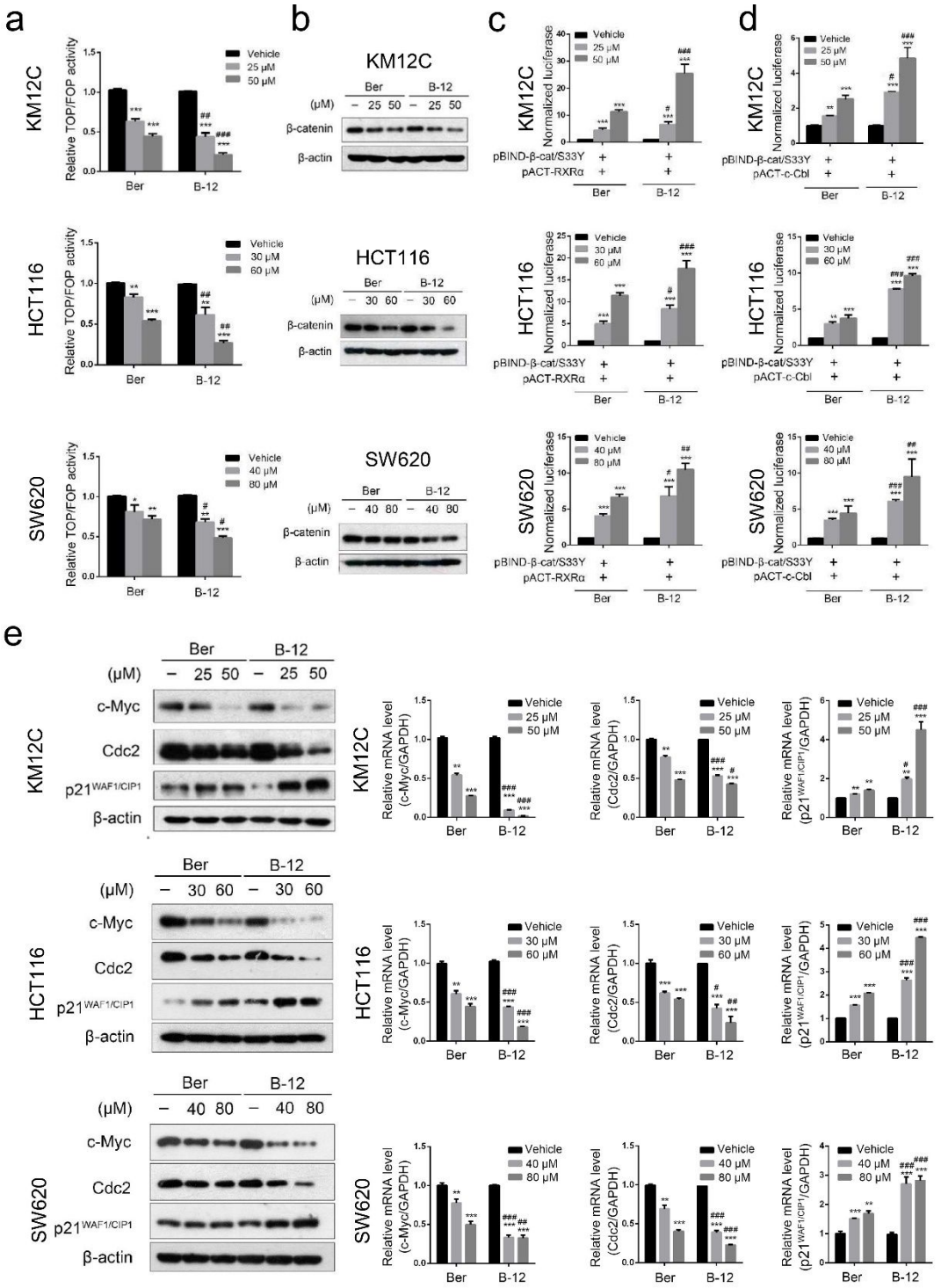

Figure 4. B-12 inhibited β-catenin signaling and cell proliferation in colon cancer cells. (**a**, **b**) Effects of berberine and **B-12** on β-catenin signaling and β-catenin expression were respectively detected by TOP/FOP luciferase system and western blot. KM12C, HCT116, and SW620 cells were co-transfected with pRL-TK, TOPflash or FOPflash plasmids (for **a**). (**c**, **d**) Effect of berberine or **B-12** on the binding ability of RXRα with β-catenin or and β-catenin with c-Cbl was detected by the mammalian two-hybrid assay. KM12C, HCT116, and SW620 cells were co-transfected with pBIND-β-catenin/S33Y and pACT-RXRα (for **c**) or pBIND-β-catenin/S33Y and pACT-c-Cbl (for **d**) and then treated with berberine or **B-12** for 15 h. (**e**, **f**) Western blot analyses and real-time PCR assays were performed to detect the protein/mRNA expression of Cdc2, c-Myc, and $p21^{WAF1/CIP1}$ in KM12C, HCT116, and SW620 cells. Significant differences compared with the vehicle were indicated as $^{**}p<0.01$ and $^{***}p<0.001$. Significant differences of **B-12** *vs* **Ber** at the same dose were indicated as $^{\#}p<0.05$, $^{\#\#}p<0.01$ and $^{\#\#\#}p<0.001$.

***B-12** inhibited β-catenin signaling and colon cancer cell growth via RXRα mediation*

We reported recently that berberine suppressed colon cancer cell proliferation through binding to RXRα and promoting its interaction with nuclear β-catenin, leading to c-Cbl-mediated degradation of β-catenin.[26] Therefore, we examined the effect of **B-12** on Wnt/β-catenin signaling pathway in KM12C, HCT116, and SW620 colon cancer cell lines. **B-12** inhibited β-catenin-dependent transcriptional activity and induced degradation of β-catenin protein more obviously than berberine, as indicated by the TOP/FOP luciferase assay and western blot analysis (Figure 4a, b). Mammalian two-hybrid assay further demonstrated that the interaction of RXRα with β-catenin and β-catenin with c-Cbl was enhanced by **B-12** more effectively than berberine (Figure 4c, d). In

addition, the expression levels of Cdc2 and c-Myc, two target genes of the β-catenin signaling pathway involved in regulating the G2/M checkpoint,[43] and $p21^{WAF1/CIP1}$, a downstream effector of c-Myc for G2/M checkpoint regulation,[44] were regulated by **B-12** more significantly than berberine (Figure 4e, f). These results suggested that similar to berberine, **B-12** also promotes RXRα–β-catenin interaction and inhibits β-catenin signaling and colon cancer cell growth, but its regulatory effect is much stronger than that of berberine.

We further investigated whether RXRα is essential for **B-12** to suppress the hyperactivated β-catenin signaling and cell growth in KM12C cells. We stably knocked down the expression of RXRα in KM12C cells with a specific shRNA against RXRα (Figure 5a). Silencing RXRα expression greatly reduced the ability of **B-12** to inhibit cell growth, as detected by the MTT assay (Figure 5b). Our results also showed that the expression of β-catenin, Cdc2, c-Myc, and $p21^{WAF1/CIP1}$ were regulated by **B-12** in an RXRα-dependent manner (Figure 5c and Figure S3). These data suggested that RXRα mediated the inhibitory effect of **B-12** on β-catenin signaling and cell growth in colon cancer cells.

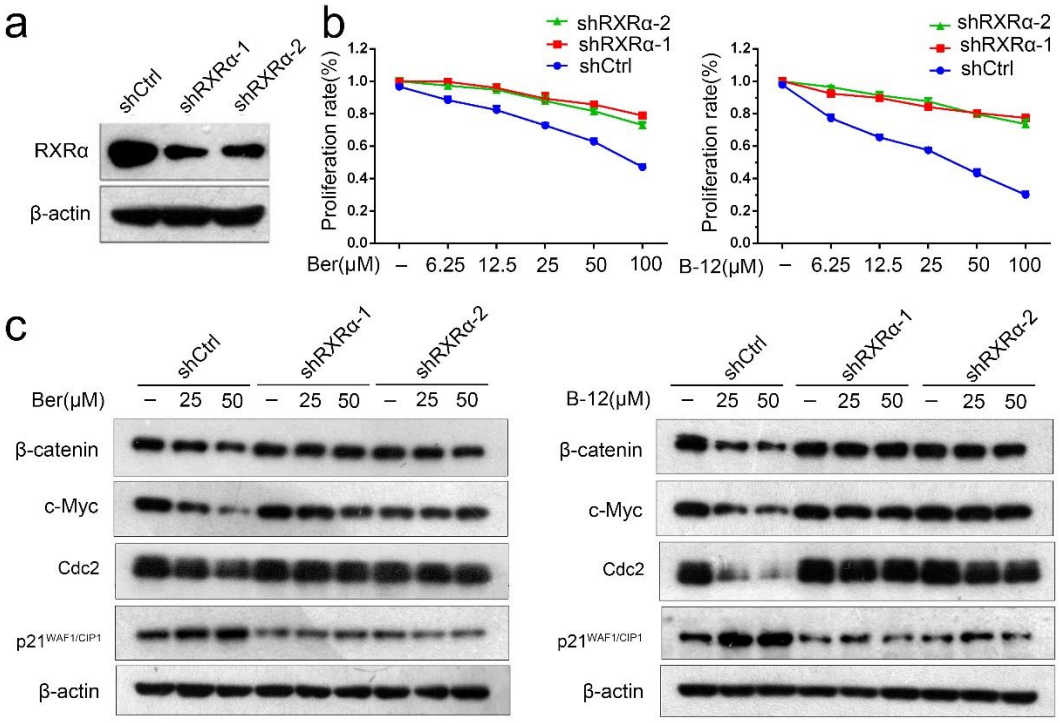

Figure 5. B-12 suppressed β-catenin signaling and cell proliferation in an RXRα-dependent manner. **(a)** KM12C cells were transfected with control shRNA or shRNA targeting RXRα, then the expression levels of endogenous RXRα were examined by western blotting analyses. **(b**, **c)** KM12C cells expressing control shRNA or shRNA targeting RXRα were treated with indicated concentrations of berberine or **B-12** for 15 h, then the cell viability was measured by MTT assays **(b)** and the protein levels of Cdc2, c-Myc and $p21^{WAF1/CIP1}$ were examined by western blot analysis **(c)**.

***B-12** inhibited tumor growth in vivo*

We assessed the therapeutic effects of **B-12** in a xenograft tumorigenesis model by subcutaneously injecting KM12C cells into nude mice. When the volume of xenografts had reached 80 to 200 mm^3, the mice with similar tumor load were divided into three groups, and then respectively treated with vehicle, **B-12** (100 mg/kg) and berberine (100 mg/kg), each day through

intragastric administration. Two weeks later, the tumors were dissected and weighed. Tumor growth was significantly reduced in **B-12**-treated and berberine-treated groups as compared to the vehicle group, and the inhibition rate was 69.1% ($P < 0.01$) and 33.6% ($P < 0.05$) for **B-12** and berberine respectively (Figure 6a-c). **B-12** also regulated the protein and mRNA expression of PCNA, Ki67, Cdc2, c-Myc, $p21^{WAF1/CIP1}$ and β-catenin in the xenograft tumors, more effectively than berberine, as detected by western blot, real-time PCR and immunohistochemistry (Figure 6d-f and Figure S4, 5). These results indicated that **B-12** inhibited colon cancer cell growth more efficiently than berberine *in vivo*.

Unwanted side effects, such as hypertriglyceridemia, mucosal toxicity, hypercalcemia and hepatomegaly, are the major obstacles of the clinical applications of current RXRα ligands. So we also tested the possible toxicity or side effects of **B-12**. Berberine and **B-12** had no obvious hepatotoxicity and nephrotoxicity as indicated by the biochemical indexes of liver and renal function measured from the serum of mice after drug treatment (Table 3). The conclusion was further supported by the results from HE staining as no damaged hepatocellular morphology and augmented necrotic hepatocytes were observed (Figure 6g). The liver to body weight ratio also proved that berberine and **B-12** did not cause hepatomegaly (Figure S6). Moreover, unlike the classical RXRα agonists, **B-12** did not cause unwanted side effects such as hypertriglyceridemia, hypercalcemia and hypercholesterolemia (Table 3).

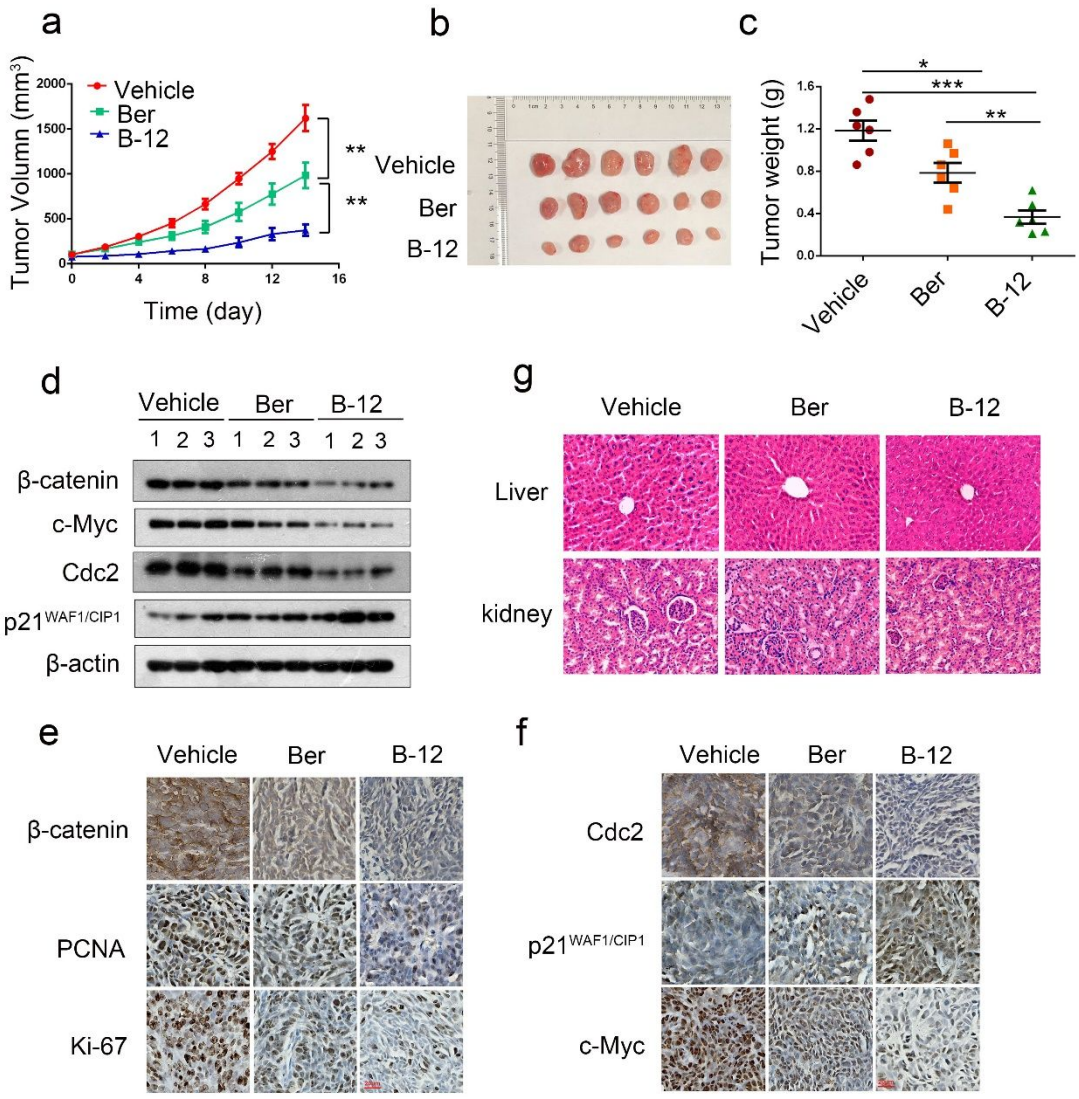

Figure 6. B-12 inhibited tumor growth in mice. Mice xenografted with KM12C cells were treated with or without berberine or **B-12** as described in the method. (**a**) Tumor volume was measured every 2 days. (**b-c**) Two weeks later, mice were sacrificed and the xenograft tumors were dissected and weighed. Representative images of tumors were shown in **b**. (**d**) Expression levels of β-catenin, Cdc2, c-Myc, and $p21^{WAF1/CIP1}$ in xenografts were analyzed by western blot. (**e**, **f**) Representative images of the expression of β-catenin, Ki-67, Cdc2, c-Myc, PCNA and $p21^{WAF1/CIP1}$ in xenograft tumors analyzed by immunohistochemistry. (**g**) Liver and kidney histopathology by HE staining.

Table 3. Biochemical analyses of the serums from berberine or B-12 treated mice

Biochemical indexes	Vehicle (n=6)	Ber (n=6)	B-12 (n=6)	*P* values Ber VS Vehicle	*P* values B12 VS Vehicle
TBIL (μmol/L)	0.28±0.024	0.26±0.032	0.21±0.029	0.4713	0.9617
IBIL (μmol/L)	0.55±0.096	0.40±0.057	0.52±0.083	0.8605	0.2423
ALT (U/L)	24.18±0.77	27.90±1.21	27.20±1.57	0.1635	0.2958
AST (U/L)	157.15±8.41	177.86±7.88	158.36±6.68	0.2239	0.9143
ALP (U/L)	76.53±4.31	71.28±3.16	78.35±5.99	0.8728	0.8739
CREA (μmol/L)	27.02±1.22	24.36±1.68	28.95±1.40	0.4813	0.6713
UREA (mmol/L)	8.21±0.26	8.08±0.62	8.39±0.41	0.8449	0.7600
Ca (mmol/L)	2.27±0.059	2.13±0.034	2.23±0.021	0.1413	0.9079
TG (mmol/L)	0.96±0.056	0.77±0.069	0.74±0.031	0.1241	0.0574
TC(mmol/L)	2.32±0.11	2.35±0.12	2.49±0.087	0.9908	0.9991

Data were presented as the mean ± SEM. Statistical significance is analyzed by one-way analysis of variance (ANOVA). P <0.05 was considered statistically significant.

*Detection of tumor selectivity and bioavailability of **B-12***

Berberine has a significant advantage of high tumor selectivity (killing tumor cells but not normal cells), which makes it a promising anti-tumor drug. Therefore, we tested whether **B-12** could still retain this advantage of berberine, by detecting the cell viability in response to a series of concentrations of **B-12** and berberine in human normal intestinal epithelial cell line HIEC-6 and

mouse fibroblast epithelial cell line MEF. Treatment with **B-12** or berberine caused only a slight decrease in viability of HIEC-6 and MEF cells, suggesting that **B-12** still preserved the high tumor selectivity of berberine (Figure 7a-b). Poor solubility and low bioavailability are two major weaknesses of berberine. Excitingly, the solubility of **B-12** was increased to 10.66 times compared with berberine (Supplementary Table 1). The increasing solubility of **B-12** is probably due to the decreasing intermolecular π, π-interaction caused by the more bulky C-3 methoxy group. We thus test whether the bioavailability of **B-12** is also better than berberine. SD rats were treated with berberine (100 mg/kg) or **B-12** (100 mg/kg) by gavage, then the blood was taken from the tail vein at different periods, and the drug concentration in the blood was detected by LC-MS. The results showed that both berberine and **B-12** reached the maximum drug concentration at approximately 2 hours, but the maximum drug concentration of **B-12** was 167 times higher than that of berberine in the blood of rats (Figure 7c and Table 4). The results of the pharmacokinetic parameters of berberine and **B-12** were shown in Table 4. Compared with berberine, the peak concentration (Cmax) was increased to 167.5 times; the area under the curve (AUC) was increased to 21.25 times; the bioavailability (F%) of **B-12** was raised to 26.10 times (Table 4), which might also contribute to B-12's stronger *in vivo* inhibitory effect on tumor growth. These results indicate that **B-12** not only reserves the high tumor selectivity of berberine but also greatly improves its bioavailability.

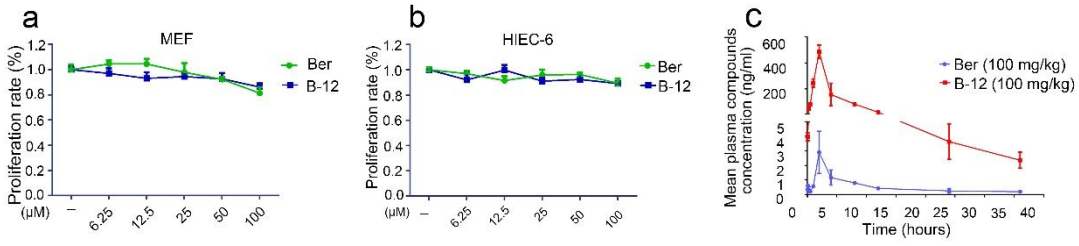

Figure 7. Detection of tumor selectivity and bioavailability of **B-12**. **(a**, **b)** MEF and HIEC-6 cells were treated with berberine or **B-12** for 15 h. The viability of cells was determined by MTT assay. (**c**) Berberine (100 mg/kg) or **B-12** (100 mg/kg) were given to SD rats by intragastric administration, and plasma samples were collected at 0.038, 0.25, 0.5, 1, 2, 4, 6, 8, 12, 24 and 36 h for analyses of berberine and **B-12** by LC-MS.

Table 4. The pharmacokinetic parameters of berberine and B-12 (PO 100mg/kg)

Compound	Ber	B-12
$T_{1/2}$ (h)	28.98	11.59
T_{max} (h)	2.000	2.000
C_{max} (ng/mL)	2.893	486.0
AUC_{0-t} (ng·h/mL)	99.00	2104
MRT_{INF} (h)	31.51	15.67
F%	0.544	14.20

■ DISCUSSION AND CONCLUSIONS

Many studies have identified RXRα as an important target for cancer therapy, especially in colon cancer.[5, 45-48] We recently reported that berberine inhibits colon cancer cell growth through direct binding to a unique site (non-classical ligand-binding pocket) in RXRα/LBD to activate its transactivating function and its regulation on β-catenin pathway.[26] To obtain more efficient berberine analogues as RXRα activators, which are very likely to retain the advantage of berberine, we designed and synthesized a series of novel berberine analogues with modifications on the C2,

3, 9, 10, 11 and 12 positions of berberine core based on its binding mode with RXRα (Figure 1-2). By analyzing the structure-activity relationship of berberine analogues and RXRα, we identified **B-12** as an effective analogue with stronger anticancer activity, comparative tumor selectivity, and significantly improved bioavailability, notably with no adverse side effects caused by traditional RXRα agonists, and no obvious toxicity to mice, which made it a promising therapeutic agent for colon cancer treatment. (Figure 2-7).

Through structure-bioactivity analysis, we have summarized the important relationships between the structural components of berberine analogues and their binding and activation of RXRα. First, the presence of particular groups on the C2, C3 positions (the head moiety) of berberine to form H-bonds with the Arg371 residue of RXRα may be required. Single C3 methoxy group or C2-C3 methylene-dioxy group can easily and closely interact with RXRα through formation of H-bonds with RXRα Arg371, and consequently exhibiting superior bio-activities in the activation of RXRα and the inhibition of colon cancer cell growth; moreover, single C3 methoxy group is a little more favorable than the C2-C3 methylenedioxy group probably due to its less steric hindrance; however, the coexistence of C2 methoxy and C3 methoxy groups with larger steric hindrance seems to prevent the compound from approaching and forming H-bonds with RXRα Arg371, thereby failing to activate RXRα and suppress colon cancer. Second, the presence of single C9 or C10 methoxy group, C10-C11 methylenedioxy group or C9/C10 bismethoxy groups on the tail region of berberine may be necessary to make maximal interaction with the hydrophobic groups in the Site X of RXRα/LBD through Van Der Waals contacts; while the presence of 10,11-dimethoxy groups or single C12 methoxy group led to poor RXRα binding potential and biological activity, which may be attributed to the unfavorable steric effect. These features may help guide the further improvement of current compounds.

As we mentioned above, berberine binds RXRα in a unique mode. Unlike other RXRα ligands such as 9-*cis*-RA, berberine lacks a classic carboxyl group which is crucial for 9-*cis*-RA to interact with RXRα through forming a salt bridge with Arg316 in the classical ligand-binding mode of RXRα[49]. These distinct structures and binding modes of berberine and 9-*cis*-RA lead to different conformational changes of RXRα and consequently some diverse biological functions. Furthermore, the concomitant binding of berberine and 9-*cis*-RA to RXRα/LBD is possibly the main reason for their synergistic effect on RXRα-dependent transcriptional activity and colon cancer cell growth, suggesting a great potential for the combination of berberine and 9-*cis*-RA to treat colon cancer[26]. Indeed, combination therapy with different drugs for cancer has long been a successful way to increase drug efficacy, reduce toxicity and reverse drug resistance. For instance, clinical trials have proven that the combination of all-*trans* retinoic acid and arsenic trioxide is a feasible treatment in acute promyelocytic leukemia with a higher cure rate and less relapse[50]. In the present study, **B-12** combined with 9-*cis*-RA had a more significant synergistic effect than berberine with 9-*cis*-RA (Figure S7), suggesting that **B-12** might be a better drug than berberine for combined drug therapy. Besides, in mouse model we also found that, unlike other RXRα ligands, **B-12** did not show side effects such as hypertriglyceridemia, hypercalcemia, and hypercholesterolemia (Table 3), which are the main reasons for the limited use of the existing RXRα agonists in clinical practice; moreover, B-12 did not induce obvious hepatorenal toxicity or hepatomegaly as most anti-tumor drugs did (Table 3, Figure 6 and Figure S6). Further studies, including *in vitro* and *in vivo* experiments, are still required to elucidate its potential.

In conclusion, this study describes a novel SAR design of berberine analogues based on the structural features of berberine analogues as RXRα activators, which might serve as a theoretical basis for designing and evaluating the next generation of berberine-based drugs against colon

cancer. Especially, we developed **B-12** as a better RXRα activator than berberine, with stronger anticancer activity, higher bioavailability, and comparative tumor selectivity.

■ EXPERIMENTAL SECTION

Chemistry

All reactions were carried out under an argon atmosphere with dry solvents under anhydrous conditions unless otherwise stated. All the chemicals were purchased commercially and used without further purification unless otherwise stated. The boiling point of petroleum ether (PE) is between 60-90 ºC. Tetrahydrofuran (THF) was distilled from sodium-benzophenone; Dichloromethane (CH_2Cl_2) was distilled from calcium hydride. Toluene was distilled from sodium under argon atmosphere. Reactions were monitored by thin-layer chromatography (TLC) carried out on 0.25 mm Qingdao silica gel plates (F254) using UV lights as the visualizing agent and $KMnO_4$. Flash column chromatography was performed over Qingdao silica gel (200-300 mesh). Infrared spectra were recorded on a Nicolet AVATER FTIR330 spectrometer as thin film and are reported in reciprocal centimeter (cm^{-1}). High-resolution mass spectra (HRMS) were recorded on a Micromass QTOF2 Quadrupole/Time-of-Flight Tandem mass spectrometer using electron spray ionization. NMR spectra were recorded on Bruker AV-400 and Bruker AV-500 instruments and were calibrated using residual undeuterated solvents ($CHCl_3$, δ_H = 7.26; DMSO-d_6, δ_H = 2.50; CD_3OD, δ_H = 3.31) and deuterated solvents ($CDCl_3$, δ_C = 77.0; CD_3OD, δ_C = 49.0; DMSO-d_6, δ_C = 39.5) as internal references. The data for ^1H NMR are reported as follows: chemical shift, multiplicity (s = singlet, d = doublet, t = triplet, m = multiplet or unresolved, brs = broad singlet), coupling constants (Hz) and integration. The structure and purity of B1-B15 was determined by qNMR with triphenylmethane as an internal standard. The purity of key compounds (**B-2**, **B-8**, **B-**

9, **B-10**, **B-12**) were also analyzed by HPLC. The purity of all the compounds were determined to be > 95%.

*General Synthetic Procedures for the Berberine Analogues **B1-B15** (**B-12** as an Example)*

*2-(2-Bromo-6-methoxyphenyl)-1,3-dioxolane (**5a**).* With a modified Donohoe's procedure: To a stirred mixture of 2-bromo-6-methoxybenzaldehyde (2.15 g, 10.0 mmol) and ethylene glycol (2.78 mL, 50 mmol) in toluene (200 mL) was added $HC(OEt)_3$ (5.0 mL, 30.0 mmol) and *p*-TSA (190 mg, 1.0 mmol) in sequence. The resultant mixture was heated at 90 °C for 18 h and then cooled to room temperature and extracted with Et_2O. The combined layers were washed with saturated brine, dried over $MgSO_4$ and concentrated *in vacuo*. Purification of the residue by flash chromatography (PE/EtOAc = 10:1) afforded **5a** as a colorless oil (2.56 g, 99%). ^1H NMR (500 MHz, $CDCl_3$) δ 7.17 – 7.14 (m, 1H), 7.10 (dd, *J* = 10.6, 5.6 Hz, 1H), 6.83 (dd, *J* = 8.2, 1.0 Hz, 1H), 6.44 (s, 1H), 4.27 – 4.19 (m, 2H), 4.01 – 3.96 (m, 2H), 3.78 (s, 3H). ^{13}C NMR (125 MHz, $CDCl_3$) δ 159.7, 130.8, 126.1, 123.7, 123.5, 110.7, 101.1, 65.7, 55.9. HRMS (ESI, m/z) calcd for $C_{10}H_{11}BrO_3$, $[M]^+$: 257.9892, found: 257.9898.

*3-Methoxyphenethyl pivalate (**2a**).* To a solution of 3-methyoxyphenylacetic acid (1.66 g, 10.0 mmol) in THF at 0 °C was added borane-THF complex solution (20.0 mL, 20.0 mmol). The mixture was allowed to warm to room temperature and stirred for 2 h before being quenched with 1 M aqueous solution of NaOH. The resulting mixture was extracted with Et_2O. The combined organic layers were washed with saturated brine, dried over $MgSO_4$ and concentrated *in vacuo*. The residue was redissolved in CH_2Cl_2 (50 mL) and cooled to 0 °C. To the mixture was added pyridine (0.8 mL, 20.0 mmol) and pivaloyl chloride (2.78 mL, 20.0 mmol) sequentially. The resulting mixture was allowed to warm to room temperature and stirred for 18 h. The reaction was

quenched with H_2O (5 mL) and extracted with CH_2Cl_2. The combined organic layers were washed with saturated brine, dried over $MgSO_4$ and concentrated *in vacuo*. Purification of the residue by flash chromatography (PE/EtOAc = 20:1) afforded **2a** as a colorless oil (2.12 g, 90%). ^{1}H NMR (500 MHz, $CDCl_3$) δ 7.17 (t, J = 7.75 Hz, 1H), 6.78 (d, J = 7.6 Hz, 1H), 6.77 – 6.72 (m, 2H), 4.25 (t, J = 6.8 Hz, 2H), 3.75 (s, 3H), 2.88 (t, J = 6.8 Hz, 2H), 1.15 (s, 9H). ^{13}C NMR (125 MHz, $CDCl_3$) δ 178.1, 159.5, 139.3, 129.2, 121.1, 114.4, 111.7, 64.6, 54.8, 38.6, 35.0, 26.9. HRMS (ESI, m/z) calcd for $C_{14}H_{20}O_3$, $[M+H]^+$: 237.1491, found: 237.1487.

*2-Acetyl-5-methoxyphenethyl pivalate (**3a**)*. To a solution of **2a** (1.89 g, 8.0 mmol) in acetic anhydride (20 mL) at 0 °C was added $ZnCl_2$ (5.45 g, 40.0 mmol). The mixture was allowed to room temperature and stirred for 18 h. The solution was concentrated *in vacuo* and then the residue was redissolved in EtOAc. The mixture was washed with saturated aqueous solution of $NaHCO_3$, water and brine. The organic phase was dried over $MgSO_4$ and concentrated *in vacuo*. Purification of the residue by flash chromatography (PE/EtOAc = 10:1) afforded **3a** as a colorless oil (1.66g, 75%). ^{1}H NMR (500 MHz, $CDCl_3$) δ 7.78 (d, J = 8.5 Hz, 1H), 6.82 – 6.76 (m, 2H), 4.30 (t, J = 6.6 Hz, 2H), 3.84 (s, 3H), 3.26 (t, J = 6.6 Hz, 2H), 2.56 (s, 3H), 1.14 (s, 9H). ^{13}C NMR (125 MHz, $CDCl_3$) δ 199.1, 178.3, 151.4, 146.8, 133.4, 129.3, 114.9, 113.5, 64.8, 55.8, 38.6, 33.6, 29.1, 27.1. HRMS (ESI, m/z) calcd for $C_{16}H_{22}O_4$, $[M+Na]^+$: 301.1416, found: 301.1410.

*2-(2-(2-(1,3-Dioxolan-2-yl)-3-methoxyphenyl)acetyl)-5-methoxyphenethyl pivalate (**6a**)*. To a stirred solution of 5a (596 mg, 2.3 mmol) and **3a** (1.28 g, 4.6 mmol) in THF (10 mL) in a 30 mL vial was added Cs_2CO_3 (1.87 g, 5.75 mmol) and $(Amphos)_2PdCl_2$ (81 mg, 0.115 mmol). The resulting solution was bubbled with argon for a minimum of 10 min and then quickly equipped with a Teflon septum. The mixture was heated at 90 °C for 18 h. The mixture was then cooled to room temperature and quenched with water and extracted with Et_2O. The combined organic layers

were washed with saturated brine, dried over $MgSO_4$ and concentrated *in vacuo*. Purification of the residue by flash chromatography (PE/EtOAc = 4:1) afforded **6a** as a colorless oil (756 mg, 72%). ^{1}H NMR (500 MHz, $CDCl_3$) δ 7.90 – 7.85 (m, 1H), 7.34 – 7.28 (m, 1H), 6.87 – 6.77 (m, 4H), 6.24 (s, 1H), 4.40 (s, 2H), 4.33 (t, *J* = 6.6 Hz, 2H), 3.84 (s, 3H), 3.81 (s, 3H), 3.80 – 3.75 (m, 2H), 3.74 – 3.67 (m, 2H), 3.24 (t, *J* = 6.6 Hz, 2H), 1.15 (s, 9H). ^{13}C NMR (125 MHz, $CDCl_3$) δ 198.7, 178.5, 161.5, 159.0, 142.2, 137.1, 131.7, 130.3, 129.9, 125.4, 121.2, 117.9, 111.5, 109.9, 98.7, 64.9, 64.5, 55.8, 55.3, 44.9, 38.7, 34.1, 27.3. HRMS (ESI, m/z) calcd for $C_{26}H_{32}O_7$, $[M+H]^+$: 457.2226, found: 457.2221.

*3,9-Dimethoxy-5,6-dihydroisoquinolino[3,2-a]isoquinolin-7-ium chloride (**B-12**).* To **6a** (723 mg, 1.58 mmol) in a 15 mL vial was added 1 M solution of NH_4Cl in 3:1 of EtOH/H_2O (4 mL). The solution was bubbled with argon for a minimum of 10 min and quickly equipped with a Teflon septum. The stirred mixture was heated at 90 °C for 18 h. Then the solution was heated at 110 °C for another 48 h. The mixture was cooled to room temperature, and concentrated with silica gel *in vacuo*. Purification of the residue by flash chromatography (CH_2Cl_2/MeOH = 10:1) afforded a crude product. The crude product was recrystallized in methanol/Et_2O to give **B-12** as a pale yellow solid (368 mg, 71%). The purity of the title compound was determined to be > 95% by qNMR. ^{1}H NMR (500 MHz, DMSO-d_6) δ 9.92 (s, 1H), 8.96 (s, 1H), 8.21 (d, *J* = 8.8 Hz, 1H), 8.11 (t, *J* = 8.1 Hz, 1H), 7.78 (d, *J* = 8.3 Hz, 1H), 7.38 (d, *J* = 7.9 Hz, 1H), 7.12 (dd, *J* = 8.7, 2.6 Hz, 1H), 7.08 (d, *J* = 2.5 Hz, 1H), 4.94 (t, *J* = 6.3 Hz, 2H), 4.13 (s, 3H), 3.88 (s, 3H), 3.31 – 3.26 (m, 2H). ^{13}C NMR (125 MHz, DMSO-d_6) δ 171.5, 166.7, 155.0, 149.8, 148.8, 147.9, 147.1, 137.7, 128.9, 128.8, 128.2, 127.2, 123.9, 122.7, 118.2, 66.2, 65.2, 64.3, 36.1. HRMS (ESI, m/z) calcd for $C_{19}H_{18}NO_2$, $[M]^+$: 292.1332, found: 292.1329.

*5,6-Dihydro-[1,3]dioxolo[4,5-g]isoquinolino[3,2-a]isoquinolin-7-ium chloride (**B-1**).* This compound was prepared from 2-bromobenzaldehyde and 2-(benzo[d][1,3]dioxol-5-yl)acetic acid using the above method. The purity of the title compound was determined to be > 95% by qNMR. ^{1}H NMR (500 MHz, $CDCl_3$) δ 8.44 – 8.39 (m, 1H), 7.62 (ddd, *J* = 8.3, 7.1, 1.3 Hz, 1H), 7.55 – 7.51 (m, 1H), 7.43 (ddd, *J* = 8.2, 7.1, 1.2 Hz, 1H), 7.26 (d, *J* = 1.6 Hz, 2H), 6.84 (s, 1H), 6.72 (s, 1H), 6.01 (s, 2H), 4.36 – 4.32 (m, 2H), 2.93 – 2.89 (m, 2H). ^{13}C NMR (125 MHz, $CDCl_3$) δ 162.1, 148.7, 147.4, 137.4, 136.7, 132.2, 130.3, 127.9, 126.2, 126.0, 124.6, 123.7, 107.9, 105.0, 101.8, 101.5, 39.7, 28.5. ^{1}H NMR (500 MHz, DMSO-d_6) δ 10.09 (d, *J* = 14.6 Hz, 1H), 9.04 (s, 1H), 8.43 (d, *J* = 8.3 Hz, 1H), 8.24 (d, *J* = 8.3 Hz, 1H), 8.19 (t, *J* = 7.6 Hz, 1H), 7.97 (t, *J* = 7.5 Hz, 1H), 7.87 (s, 1H), 7.11 (s, 1H), 6.18 (s, 2H), 4.88 (t, *J* = 6.0 Hz, 2H), 3.24 (t, *J* = 6.3 Hz, 2H). ^{13}C NMR (125 MHz, DMSO-d_6) δ 150.4, 148.3, 147.8, 141.7, 138.4, 137.5, 136.7, 134.4, 131.1, 130.5, 129.9, 129.2, 127.2, 125.5, 120.5, 120.4, 114.3, 108.5, 106.4, 105.8, 105.1, 102.2, 55.2, 26.3. HRMS (ESI, m/z) calcd for $C_{18}H_{14}NO_2$, $[M]^+$: 276.1019, found: 276.1016. Spectroscopic date were consistent with those previously reported.[42]

*5,6-Dihydro-[1,3]dioxolo[4',5':6,7]isoquinolino[3,2-a][1,3]dioxolo[4,5-g]iso quinolin-7-ium chloride (**B-2**, pseudocoptisine).* This compound was prepared from 6-bromobenzo[d][1,3]dioxole-5-carbaldehyde and 2-(benzo[d][1,3]dioxol-5-yl)acetic acid using the above method. The purity of the title compound was determined to be > 95% by qNMR. ^{1}H NMR (400 MHz, DMSO-d_6) δ 9.57 (s, 1H), 8.77 (s, 1H), 7.74 (s, 1H), 7.71 (s, 1H), 7.54 (s, 1H), 7.09 (s, 1H), 6.42 (s, 2H), 6.17 (s, 2H), 4.76 (t, *J* = 6.4 Hz, 2H), 3.18 (t, *J* = 6.4 Hz, 2H). ^{13}C NMR (100 MHz, DMSO-d_6) δ 156.4, 151.3, 150.4, 148.1, 146.3, 139.2, 139.1, 131.3, 124.0, 120.7, 119.4, 108.9, 105.9, 104.3, 104.2, 103.1, 102.5, 54.9, 26.8. HRMS (ESI, m/z) calcd for $C_{19}H_{14}NO_4$, $[M]^+$: 320.0917, found: 320.0915. Spectroscopic date were consistent with those previously reported.[37]

*3,10,11-Trimethoxy-5,6-dihydroisoquinolino[3,2-a]isoquinolin-7-ium chloride (**B-3**).* This compound was prepared from 2-bromo-4,5-dimethoxybenzaldehyde and 2-(3-methoxyphenyl)acetic acid using the above method. The purity of the title compound was determined to be > 95% by qNMR.^{1}H NMR (500 MHz, CD_3OD) δ 9.35 (s, 1H), 8.59 (s, 1H), 8.09 (d, J = 8.8 Hz, 1H), 7.62 (s, 1H), 7.60 (s, 1H), 7.09 (dd, J = 8.8, 2.5 Hz, 1H), 7.03 (d, J = 2.5 Hz, 1H), 4.82 (t, J = 6.6 Hz, 2H), 4.12 (s, 3H), 4.06 (s, 3H), 3.91 (s, 3H), 3.32 (t, J = 6.6 Hz, 2H). ^{13}C NMR (125 MHz, CD_3OD) δ 162.6, 158.5, 153.1, 144.6, 139.2, 137.6, 136.9, 127.4, 122.8, 119.4, 117.7, 114.4, 113.0, 105.9, 104.9, 56.1, 55.7, 54.8, 54.7, 27.2. HRMS (ESI, m/z) calcd for $C_{20}H_{20}NO_3$, $[M]^+$: 322.1438, found: 322.1435.

*10,11-Dimethoxy-5,6-dihydro-[1,3]dioxolo[4,5-g]isoquinolino[3,2-a]isoquin olin-7-ium chloride (**B-4**, pseudoberberine).* This compound was prepared from 2-bromo-4,5-dimethoxybenzaldehyde and 2-(benzo[d][1,3]dioxol-5-yl)acetic acid using the above method. The purity of the title compound was determined to be > 95% by qNMR.^{1}H NMR (500 MHz, DMSO-d_6) δ 9.57 (s, 1H), 8.77 (s, 1H), 7.73 (s, 1H), 7.72 (s, 1H), 7.59 (s, 1H), 7.10 (s, 1H), 6.17 (s, 2H), 4.78 (t, J = 6.3 Hz, 2H), 4.07 (s, 3H), 4.00 (s, 3H), 3.20 (t, J = 6.3 Hz, 2H). ^{13}C NMR (125 MHz, DMSO-d_6) δ 157.5, 152.3, 149.8, 147.7, 145.5, 138.2, 136.6, 130.7, 122.1, 118.2, 108.5, 106.6, 105.3, 102.1, 56.7, 56.4, 54.5, 26.4. HRMS (ESI, m/z) calcd for $C_{20}H_{18}NO_4^+$, $[M]^+$: 336.1236, found: 336.1234. Spectroscopic date were consistent with those previously reported.[51]

*2,3,10,11-Tetramethoxy-5,6-dihydroisoquinolino[3,2-a]isoquinolin-7-ium chloride (**B-5**, pseudopalmatine).* This compound was prepared from 2-bromo-4,5-dimethoxybenzaldehyde and 2-(3,4-dimethoxyphenyl)acetic acid using the above method. The purity of the title compound was determined to be > 95% by qNMR.^{1}H NMR (500 MHz, DMSO-d_6) δ 9.58 (s, 1H), 8.88 (s, 1H), 7.72 (s, 1H), 7.67 (s, 1H), 7.62 (s, 1H), 7.10 (s, 1H), 4.80 (t, J = 6.3 Hz, 2H), 4.08 (s, 3H), 4.00 (s,

3H), 3.94 (s, 3H), 3.87 (s, 3H), 3.22 (t, J = 6.3 Hz, 2H). ^{13}C NMR (125 MHz, DMSO-d_6) δ 157.4, 152.2, 151.5, 148.7, 145.6, 138.4, 136.6, 128.6, 122.0, 118.9, 118.0, 111.3, 108.5, 106.5, 105.3, 56.6, 56.3, 56.0, 55.9, 54.6, 26.1. HRMS (ESI, m/z) calcd for $C_{21}H_{22}NO_4$, $[M]^+$: 352.1543, found: 352.1540. Spectroscopic date were consistent with those previously reported.[51]

*2,3-Dimethoxy-5,6-dihydroisoquinolino[3,2-a]isoquinolin-7-ium chloride (**B-6**)*. This compound was prepared from 2-bromobenzaldehyde and 2-(3,4-dimethoxyphenyl)acetic acid using the above method. The purity of the title compound was determined to be > 95% by qNMR. ^{1}H NMR (500 MHz, CD_3OD) δ 9.81 (s, 1H), 8.93 (s, 1H), 8.38 (d, J = 8.3 Hz, 1H), 8.30 (d, J = 8.4 Hz, 1H), 8.17 – 8.13 (m, 1H), 7.96 – 7.92 (m, 1H), 7.72 (s, 1H), 7.07 (s, 1H), 4.95 (t, J = 6.4 Hz, 2H), 4.01 (s, 3H), 3.95 (s, 3H), 3.34 (t, J = 6.4 Hz, 2H). ^{13}C NMR (125 MHz, CD_3OD) δ 154.2, 151.1, 151.0, 142.0, 140.7, 138.0, 131.7, 131.0, 130.5, 128.6, 127.4, 121.7, 120.3, 112.3, 110.3, 57.3, 57.1, 56.7, 27.7. HRMS (ESI, m/z) calcd for $C_{19}H_{18}NO_2$, $[M]^+$: 292.1332, found: 292.1330.

*3-Methoxy-5,6-dihydroisoquinolino[3,2-a]isoquinolin-7-ium chloride (**B-7**)*. This compound was prepared from 2-bromobenzaldehyde and 2-(3-methoxyphenyl)acetic acid using the above method. The purity of the title compound was determined to be > 95% by qNMR. ^{1}H NMR (500 MHz, CD_3OD) δ 9.83 (s, 1H), 8.81 (s, 1H), 8.38 (d, J = 8.3 Hz, 1H), 8.26 (d, J = 8.4 Hz, 1H), 8.16 – 8.09 (m, 2H), 7.94 – 7.87 (m, 1H), 7.07 (dd, J = 8.8, 2.6 Hz, 1H), 7.02 (d, J = 2.5 Hz, 1H), 4.95 (t, J = 6.3 Hz, 2H), 3.89 (s, 3H), 3.36 (t, J = 6.3 Hz, 2H). ^{13}C NMR (125 MHz, CD_3OD) δ 164.2, 151.0, 142.0, 140.6, 138.5, 138.0, 131.6, 131.0, 129.4, 128.5, 127.3, 121.4, 120.6, 116.0, 114.3, 57.0, 56.3, 28.4. HRMS (ESI, m/z) calcd for $C_{18}H_{16}NO$, $[M]^+$: 262.1226, found: 262.1224.

*3-Methoxy-5,6-dihydro-[1,3]dioxolo[4,5-g]isoquinolino[2,1-b]isoquinolin-7-ium chloride (**B-8**)*. This compound was prepared from 6-bromobenzo[d][1,3]dioxole-5-carbaldehyde and 2-(3-methoxyphenyl)acetic acid using the above method. The purity of the title compound was

determined to be > 95% by qNMR.^{1}H NMR (500 MHz, DMSO-d_6) δ 9.57 (s, 1H), 8.79 (s, 1H), 8.11 (d, J = 8.7 Hz, 1H), 7.71 (s, 1H), 7.60 (s, 1H), 7.12 (dd, J = 8.7, 2.3 Hz, 1H), 7.08 (d, J = 2.2 Hz, 1H), 6.41 (s, 1H), 4.79 (t, J = 6.0 Hz, 2H), 3.88 (s, 3H), 3.27 (t, J = 6.0 Hz, 2H). ^{13}C NMR (125 MHz, DMSO-d_6) δ 164.1, 158.3, 153.0, 146.5, 141.2, 138.4, 129.0, 125.6, 120.6, 119.9, 119.8, 115.8, 114.4, 105.4, 104.7, 103.9, 64.3, 56.2, 28.4. HRMS (ESI, m/z) calcd for $C_{19}H_{16}NO_3$, $[M]^+$: 306.1125, found: 306.1121.

*10-Methoxy-5,6-dihydro-[1,3]dioxolo[4,5-g]isoquinolino[3,2-a]isoquinolin-7-ium chloride (**B-9**)*. This compound was prepared from 2-bromo-5-methoxybenzaldehyde and 2-(benzo[d][1,3]dioxol-5-yl)acetic acid using the above method. The purity of the title compound was determined to be > 95% by qNMR. ^{1}H NMR (500 MHz, DMSO-d_6) δ 9.84 (s, 1H), 8.99 (s, 1H), 8.17 (d, J = 9.1 Hz, 1H), 7.85 (dd, J = 9.1, 2.4 Hz, 1H), 7.81 (s, 1H), 7.77 (d, J = 2.4 Hz, 1H), 7.10 (s, 1H), 6.18 (s, 2H), 4.87 (t, J = 6.3 Hz, 2H), 4.00 (s, 3H), 3.22 (t, J = 6.3 Hz, 2H). ^{13}C NMR (125 MHz, DMSO-d_6) δ 160.0, 149.9, 147.8, 147.7, 138.0, 134.4, 130.6, 129.8, 129.1, 127.3, 120.4, 108.4, 106.5, 105.5, 102.1, 56.2, 55.6, 55.2, 26.3. HRMS (ESI, m/z) $C_{19}H_{16}NO_3$, $[M]^+$: 306.1125, found: 306.1122. Spectroscopic date were consistent with those previously reported.[42]

*3,9,10-Trimethoxy-5,6-dihydroisoquinolino[3,2-a]isoquinolin-7-ium chloride (**B-10**)*. This compound was prepared from 6-bromo-2,3-dimethoxybenzaldehyde and 2-(3-methoxyphenyl)acetic acid using the above method. The purity of the title compound was determined to be > 95% by qNMR.^{1}H NMR (500 MHz, DMSO-d_6) δ 8.96 (s, 1H), 8.32 (s, 1H), 8.18 (d, J = 9.2 Hz, 1H), 8.14 (d, J = 8.7 Hz, 1H), 8.04 (d, J = 9.1 Hz, 1H), 7.10 (dd, J = 8.7, 2.6 Hz, 1H), 7.07 (d, J = 2.3 Hz, 1H), 4.96 (t, J = 6.2 Hz, 2H), 4.09 (s, 3H), 4.06 (s, 3H), 3.87 (s, 3H), 3.28 (t, J = 6.2 Hz, 2H). ^{13}C NMR (125 MHz, DMSO-d_6) δ 162.0, 150.7, 145.8, 138.3, 137.6,

133.6, 128.2, 127.2, 124.0, 121.9, 120.2, 120.0, 114.9, 113.7, 79.7, 62.4, 60.2, 57.5, 56.1, 27.2. HRMS (ESI, m/z) calcd for $C_{20}H_{20}NO_3$, $[M]^+$: 322.1438, found: 322.1439.

*2,3,9,10-Tetramethoxy-5,6-dihydroisoquinolino[3,2-a]isoquinolin-7-ium chloride (**B-11**, palmatine).* This compound was prepared from 6-bromo-2,3-dimethoxybenzaldehyde and 2-(3,4-dimethoxyphenyl)acetic acid using the above method. The purity of the title compound was determined to be > 95% by qNMR.^{1}H NMR (500 MHz, CD_3OD) δ 9.73 (s, 1H), 8.76 (s, 1H), 8.06 (d, *J* = 8.8 Hz, 1H), 7.99 (d, *J* = 8.8 Hz, 1H), 7.59 (s, 1H), 7.01 (s, 1H), 4.93 (s, 2H), 4.19 (s, 3H), 4.07 (s, 3H), 3.97 (s, 3H), 3.92 (s, 3H), 3.27 (s, 2H). ^{13}C NMR (125 MHz, CD_3OD) δ 153.7, 151.8, 150.8, 146.3, 145.6, 139.7, 135.2, 130.0, 127.9, 124.5, 123.2, 121.2, 120.4, 112.2, 109.9, 62.6, 57.6, 57.3, 57.1, 56.7, 27.8. ^{1}H NMR (500 MHz, DMSO-d_6) δ 9.90 (s, 1H), 9.08 (s, 1H), 8.21 (d, *J* = 9.1 Hz, 1H), 8.04 (d, *J* = 9.1 Hz, 1H), 7.73 (s, 1H), 7.09 (s, 1H), 4.96 (t, *J* = 6.3 Hz, 2H), 4.10 (s, 3H), 4.07 (s, 3H), 3.94 (s, 3H), 3.87 (s, 3H), 3.23 (t, *J* = 6.3 Hz, 2H). ^{13}C NMR (125 MHz, DMSO-d_6) δ 151.5, 150.2, 148.7, 145.4, 143.6, 137.7, 133.1, 128.6, 126.8, 123.4, 121.3, 119.9, 118.9, 111.3, 108.8, 61.9, 57.0, 56.2, 55.9, 55.3, 26.0. HRMS (ESI, m/z) calcd for $C_{21}H_{22}NO_4$, $[M]^+$: 352.1543, found: 352.1539. Spectroscopic date were consistent with those previously reported.[37]

*2,3,9-Trimethoxy-5,6-dihydroisoquinolino[3,2-a]isoquinolin-7-ium chloride (**B-13**).* This compound was prepared from 2-bromo-6-methoxybenzaldehyde and 2-(3,4-dimethoxyphenyl)acetic acid using the above method. The purity of the title compound was determined to be > 95% by qNMR. ^{1}H NMR (500 MHz, CD_3OD) δ 9.80 (s, 1H), 8.83 (s, 1H), 7.92 (d, *J* = 8.3 Hz, 1H), 7.86 (t, *J* = 8.0 Hz, 1H), 7.63 (s, 1H), 7.56 (d, *J* = 7.7 Hz, 1H), 7.07 (s, 1H), 4.94 (t, *J* = 6.3 Hz, 2H), 4.17 (s, 3H), 4.00 (s, 3H), 3.94 (s, 3H), 3.35 (t, *J* = 6.3 Hz, 2H). ^{13}C NMR (125 MHz, CD_3OD) δ 154.5, 152.8, 149.5, 149.2, 140.1, 131.2, 129.2, 126.7, 120.7, 119.0,

114.8, 113.7, 111.0, 108.9, 55.9, 55.80, 55.4, 29.3, 26.3. HRMS (ESI, m/z) calcd for $C_{20}H_{20}NO_3$, $[M]^+$: 322.1438, found: 322.1440.

*2,3,12-Trimethoxy-5,6-dihydroisoquinolino[3,2-a]isoquinolin-7-ium chloride (**B-14**)*. This compound was prepared from 2-bromo-3-methoxybenzaldehyde and 2-(3,4-dimethoxyphenyl)acetic acid using the above method. The purity of the title compound was determined to be > 95% by qNMR.^{1}H NMR (500 MHz, CD_3OD) δ 9.82 (s, 1H), 8.81 (s, 1H), 8.07 (t, *J* = 8.1 Hz, 1H), 7.79 (d, *J* = 8.3 Hz, 1H), 7.67 (s, 1H), 7.32 (d, *J* = 8.0 Hz, 1H), 7.05 (s, 1H), 4.96 – 4.91 (m, 2H), 4.18 (s, 3H), 4.00 (s, 3H), 3.94 (s, 3H), 3.32 – 3.28 (m, 2H). ^{13}C NMR (125 MHz, CD_3OD) δ 157.8, 152.7, 149.4, 145.2, 140.7, 140.0, 138.5, 129.2, 119.5, 118.8, 118.6, 118.4, 110.9, 108.9, 108.1, 62.8, 55.9, 55.7, 55.3. HRMS (ESI, m/z) calcd for $C_{20}H_{20}NO_3$, $[M]^+$: 322.1438, found: 322.1439.

*12-Methoxy-5,6-dihydro-[1,3]dioxolo[4,5-g]isoquinolino[3,2-a]isoquinolin-7-ium chloride (**B-15**)*. This compound was prepared from 2-bromo-3-methoxybenzaldehyde and 2-(benzo[d][1,3]dioxol-5-yl)acetic acid using the above method. The purity of the title compound was determined to be > 95% by qNMR. ^{1}H NMR (500 MHz, CD_3OD) δ 9.80 (s, 1H), 8.71 (s, 1H), 7.90 (d, *J* = 8.2 Hz, 1H), 7.84 (t, *J* = 8.0 Hz, 1H), 7.58 (s, 1H), 7.54 (d, *J* = 7.7 Hz, 1H), 6.93 (s, 1H), 6.08 (s, 2H), 4.97 – 4.90 (m, 3H), 4.15 (s, 3H), 3.29 – 3.24 (m, 2H). ^{13}C NMR (125 MHz, CD_3OD) δ 154.5, 151.0, 149.2, 148.5, 139.9, 131.4, 131.2, 130.9, 126.8, 120.7, 120.3, 114.9, 113.7, 108.1, 105.3, 102.4, 55.8, 55.7, 26.7. HRMS (ESI, m/z) calcd for $C_{19}H_{16}NO_3$, $[M]^+$: 306.1125, found: 306.1121.

■ BIOLOGICAL ASSAY PROTOCOLS

Chemicals and reagents

Berberine (cat. #141433-60-5) and 9-*cis*-RA (cat. #5300-03-8) were purchased from Sigma-Aldrich, St. Louis, MO, USA. Rabbit anti-p21$^{WAF1/CIP1}$ (cat. #2947), anti-Ki67 (cat. #9449) and mouse anti-β-catenin (cat. #6582), anti-Cdc2 (cat. #9116) antibodies were purchased from Cell Signaling Technology, Boston, MA, USA. Rabbit anti-c-Myc (cat. #40764) antibodies were purchased from Signalway Antibody, Baltimore, USA. Rabbit anti-PCNA (cat. #ab2426) antibody was purchased from Abcam, Boston, MA, USA. Rabbit anti-RXRα was purchased from Santa Cruz Biotechnology, Santa Cruz, CA, USA.

Molecular docking study

To further understand the relationship between berberine (and its analogues) and protein RXRα/LBD, molecular docking simulations were performed. The 3D structure of RXRα/LBD protein was obtained from the Protein Data Bank using PDB ID: 3FUG. Then the 3D structure was prepared by removing the water molecules from the structure and defining binding sites using APOPDB2RECEPTOR utility implemented in Openeye software suits. Small molecule structures were prepared by SYBYL2.0 and conformational enumeration was done by OMEGA utility implemented in Openeye software suits, with all parameters set default. After that FRED docking tool was used for molecular docking simulations and its Chemgauss4 score was used for ranking the pose of each docked compound. Conformation with the highest score was used for further evaluation. Interaction between small molecule and protein was shown by VIDA.

Cell culture

Human colon cell lines HIEC-6 were obtained from ATCC (Virginia, USA). The colon cancer cell lines HCT116 and SW620 were obtained from Cell Bank of Type Culture Collection of

Chinese Academy of Sciences (Shanghai, China). Human KM12C colon cancer cell line, established from a Duke's B2 primary colon cancer, was kindly provided by Professor I. J. Fidler (M.D. Anderson Cancer Center, Houston, TX, USA). Mouse embryonic fibroblast MEF cell lines were kindly provided by Professor Bo-an Li (Xiamen University, China). Mycoplasma testing was regularly conducted to assure that all these cell lines were mycoplasma-free at all times. KM12C were maintained in MEM culture medium (Gibco, Grand Island, NY, USA) supplemented with 10 % fetal bovine serum (FBS, Invitrogen; Thermo Fisher Scientific), 100 IU/mL penicillin (Life Technologies, Carlsbad, CA, USA), 100 μg/mL streptomycin (Life Technologies), 1% non-essential amino acids (Gibco) and 1% vitamin solution (Gibco). HIEC-6 were maintained in MEM culture medium (Gibco, Grand Island, NY, USA) supplemented with 4 % fetal bovine serum (FBS, Invitrogen; Thermo Fisher Scientific), 100 IU/mL penicillin (Life Technologies, Carlsbad, CA, USA), 100 μg/mL streptomycin (Life Technologies), 20 mM HEPES (Gibco),10 mM GlutaMAX (Gibco Catalog No. 35050) and 10 ng/mL Epidermal Growth Factor (EGF) (Gibco). MEF cells were cultured in DMEM high-glucose medium (Gibco) prepared with 10% of fetal bovine serum, 100 IU/mL penicillin and 100 μg/mL streptomycin. All cell lines were maintained at 37 °C in an atmosphere of 95% air and 5% CO2.

Transfection and dual-luciferase reporter assays

The cells were inoculated into 24 well culture plates. After 24 h, different luciferase reporter genes and other different expression vectors as required were transfected with liposome transfection reagent Lipfectamine 2000 (Invitrogen, Gaithersburg, MD, USA) according to the manufacturer's recommendations. Luciferase assays were carried out according to the instructions of the Dual-Luciferase Reporter Assay Kit (Promega, Madison, WI, USA). Briefly, after 20 h of

transfection, berberine or berberine analogues were added for 15 h and then the medium was carefully removed. 100 μL 1× Passive Lysis Buffer was added into each hole at 4 °C for 1 h, the Firefly and renilla luciferase activity was detected by GloMax 20/20 Luminometer (Promega).

Cell proliferation assay

Cell proliferation rates were determined by MTT assay or EdU assay. In MTT assay, briefly, the cells were seeded in 96-well plates at a density of 1×10^4 cells/well. After incubated at 37 °C overnight, the cells were treated with berberine or **B-12** at different concentrations for 15 h, then 20 μL MTT (5 mg/mL) solution was added to each well and incubated for 4 h at 37 °C. Four hours later, the medium was removed carefully. 150 μL DMSO was added to each well to dissolve formazan crystals. The absorbance at 570 nm was measured using a Model 680 microplate reader (Bio-Rad, Hercules, CA, USA). The EdU assay was performed in a 96-well plate by EdU assay kit (Ribobio, China) according to the instruction, and the cells were examined under a fluorescence microscope.

Purification of His-RXRα-LBD fusion proteins

The constructed pET15b-RXR-LBD expression plasmid was transformed into Ecoli strain BL21 (DE3) to express the target protein. The strain was cultured in fresh LB medium containing ampicillin at 37 °C and 250 rpm until OD600 reached 0.6. Isopropyl-1-thio-b-D-galactopyranoside (IPTG) with final concentration of 0.1 mM was added. After 16 h of induction at 16 °C, the strain was centrifuged at 5000 rpm for 20 min to collect. The protein was purified according to the standard His-tag fusion protein method. Briefly, the bacteria were resuspended with lysis buffer (50 mM NaH_2PO_4 pH 8.0, 300 mM NaCl, 10 mM imidazole, 0.5% (v/v) Triton X-100)

supplemented with PMSF (1 mM), sonicated, and centrifuged at 10000 rpm, at 4 °C for 30 min. The supernatant was added to NiNTA resin chromatography affinity column, then incubated at 4 °C for 1 h, and washed twice with 800 μL wash buffer (50 mM NaH_2PO_4 pH 8.0, 300 mM NaCl, 50 mM imidazole). Finally, the target protein was eluted with 100 μL elution buffer (50 mM NaH_2PO_4 pH 8.0, 300 mM NaCl, 250 mM imidazole). After the purity of the collected samples was detected by discontinuous SDS-PAGE, the components with a purity of more than 90% were dialyzed into the required buffer for the following experiments.

Saturation Transfer Difference (STD) NMR experiment

The NMR samples used for STD experiment contain 600 μL 0.01 mM PBS buffer solution (pH 7.4) consisting of 10 μM RXRα/LBD, 200 μM berberine or **B-12**, 5% DMSO and 5% D_2O. All NMR experiments were performed on Bruker 800 MHz AVANCE III HD equipped with a cryoprobe at 25 °C. The Bruker pulse program stddiffgp19.3 was used to collect STD NMR data and the saturation time was set to 2 sec. The STD spectra were processed and analyzed by Topspin 3.5.

Fluorescence titration measurements

The fluorescence titration measurements were carried out on a VARIAN spectrofluorometer model Varian Eclipse. The sample quartz cuvette path length was 1 cm, and the excitation and emission slit widths were set as 5 nm. Then the fluorescence spectra of RXRα and the RXRα–berberine complex were recorded in the wavelength range 290–600 nm after excitation at 280 nm. The change in fluorescence intensity was observed by continuous stirring varying concentrations of berberine (2-30 μM) to the fixed concentration of RXRα (1 μM) in PBS buffer solution (pH

7.4). The DMSO titrated with an equal amount of berberine was also measured and subtracted from their respective samples to correct its effect. Each spectrum was measured three times.

Circular dichroism (CD) spectroscopy

CD spectra were measured with a Jasco J-810 spectropolarimeter (Jasco Corporation, Tokyo, Japan) at 25 °C. Instrument path length was set to 0.1 cm, and wavelength range at 180-260 nm (protein secondary structure). The band width was set to 1 nm with the response time of 1 s and a scanning speed of 20 nm/min. All measurements were detected in the 0.01 M phosphate buffer. Purification of His-RXRα-LBD was dilute to 1 μM in phosphate buffer, and the concentration of berberine or B-12 was 5 μM (DMSO concentration was 0.01%). For the displacement studies, the spectra were recorded 5 min after addition of the berberine to the His-RXRα/LBD solution. Average of 3 scans were collected for each spectrum.

Real-time PCR

Total RNA was extracted with Trizol (Invitrogen) reagent according to the manufacturer's instructions. Then 1 μg mRNA was reversely transcribed to cDNA by Reverse Transcription System (Promega). The mRNA expression levels of target genes were detected by LightCycler 96 Real-Time PCR System (Roche Diagnostics GmbH, Mannheim, Germany) with SYBR Premix EX Taq (TaKaRa, Japan). GAPDH gene level was set as an internal control.

The primers were listed below:

GAPDH:

Forward: 5′ - TGCACCACCAACTGCTTAGC-3′

Reverse: 5′ GGCATGGACTGTGGTCATGAG-3′ ;

c-Myc:

Forward: 5' GGGGCTTTATCTAACTCGC 3'

Reverse: 5' CTATGGGCAAAGTTTCGTG 3'

Cdc2:

Forward: 5' AAACTACAGGTCAAGTGGTAGCC3'

Reverse: 5' TCCTGCATAAGCACATCCTGA3'

$p21^{WAF1/CIP1}$:

Forward: 5'-CCACTGGAGGGTGACTTCG-3'

Reverse: 5'-TGCAGCAGAGCAGGTGAGG-3'

RXRα shRNA

The lentiviral vector-based shRNA technique was used to knockdown endogenous RXRα in KM12C cells. The targeted sequences of human RXRα shRNA was 5′-GTGTTGTCACCCTCCTTATTT-3′; 5′-CCTGTCTGGAGTGACATCT -3′. The negative control shRNA sequence was 5′-GGCTACGTCCAGGAGCGCACC-3′.

Mouse xenograft models

Male six-week-old nude mice (BALB/c, SPF grade, 19-23 g) were maintained in Xiamen University Experimental Animal Center. The mice were allowed to get accustomed to the new environment for one week before the experiment. All animal studies were handled in accordance with the Institutional Animal Use and Care Committee of Xiamen University (China). KM12C cells (1×10^6 per mouse) resuspended in 100 μL Hank's Balanced Salt Solution (HBSS) were subcutaneously injected into both flanks of nude mice. The tumor-bearing mice were randomly

divided into three groups after seven days and were then treated daily with Vehicle (Carboxymethyl Cellulose Sodium-Na, CMC-Na), berberine (100 mg/kg body weight), and **B-12** (100 mg/kg body weight) by intragastric administration daily for 15 days. Then the mice were euthanized and the tumors were removed for follow-up study.

Determination of Serum biochemical indexes

Serum samples were collected from mice and the following biochemical indexes were measured: liver function indexes (Bilirubin total (TBIL), indirect Bilirubin (IBIL), alanine aminotransferase (ALT), aspartate aminotransferase (AST), and alkaline phosphatase (ALP); kidney function indexes (urea formaldehyde (UREA), and creatinine (CREA)); glycolipid function indexes (total cholesterol (TC), and triglyceride (TG)); and Calcium (Ca) concentration. All the indexes were measured by using Automatic Chemistry Analyzer（BS-240vet, Mindray Bio-Medical Electronics Co., Ltd. Shenzhen, China).

Immunohistochemical assay

Tumor tissue specimens were fixed with neutral formalin and embedded in paraffin. Tissue sections (4 μm thick) were dewaxed and deparaffinized in xylene, followed by treatment with a graded series of alcohol (100, 95, 85, and 70%) and rehydration in PBS (pH 7.5). After that, tissue sections were immersed in 3% hydrogen peroxide for 10 min to suppress endogenous peroxidase activity, and then successively incubated with 0.01 M natrium citricum (pH 6.0) for antigen retrieval. The slides were rinsed in PBS (pH 7.5) and incubated with diluted antibody incubating at 4 °C overnight and performed with the immunostaining kit according to the manufacturer's

instructions. DAB Detection Kit (cat. #Kit-0014) was purchased from Maixin Biotech (Fuzhou, China).

Pharmacokinetics Study

SD rats weighed 200 ± 20 g were housed at 28 °C in a laminar flow under sterilized conditions. Rats were randomly divided into three groups and then treated with berberine (100 mg/kg), **B-12** (100 mg/kg) or vehicle (0.5% CMC-Na) by intragastric administration. Blood samples (0.5 mL) were collected via the tail vein at 0.083、0.25、0.5、1、2、4、8、12、24、36 h after intragastric administration. After centrifugation at 2000 rpm for 10 min, the resulting plasma was frozen at -80 °C until LC-MS/MS quantification. Pharmacokinetic data analyses were conducted using a noncompartmental analysis model (DAS 2.0, T.C.M., Shanghai, China). All animal procedures were approved by the Animal Care and Use Committee of Xiamen University.

Solubility measurements

The gravimetric method was used to detect the solubility of berberine and its analogues. In brief, excess amount of powder was added into 10 mL deionized water in three parallel groups for each compound. Samples were shaken at 37 °C for 24 h, and centrifuged at 10,000 rpm for 5 min. Then 5 mL supernatant was taken out and put into an evaporating dish (dried and weighed in advance, whose net weight was labeled as W1 (with the unit of grams), which was subsequently placed in the oven at 60 °C until the weight became constant. The total mass of the compound and the evaporating dish was then weighed (in the accuracy of 0.0001 g) and labeled as W2 (with the unit of grams). The solubility of berberine and berberine analogues in water (mg/mL) is calculated

according to the following formula: $X = (W2-W1)/5\times10^3$, in which 5 is the volume of the supernatant (mL).

Statistical analyses

All results are shown as mean ± SEM. Statistical significance is analyzed by one-way or two-way ANOVA by GraphPad Prism software (version 5.0, GraphPad Software Inc., La Jolla, CA, USA). The statistical significance was expressed as $*p < 0.05$, $**p < 0.01$ and $***p< 0.001$.

■ ABBREVIATIONS

Retinoid X receptor α (RXRα); structure-activity analysis (SAR); adenomatous polyposis coli (APC); ligand-binding pocket (LBP); ligand-binding domian (LBD); 9-*cis*-retinoid acid (9-*cis*-RA); berberine (Ber); hydrogen bonds (H-bonds); 5-Ethynyl-2'-deoxyuridine (EdU); proliferating cell nuclear antigen (PCNA); saturation transfer difference (STD); nuclear magnetic resonance (NMR); far-ultraviolet circular dichroism spectrum (far-UV CD spectrum); area under the curve (AUC)

■ ACKNOWLEDGMENTS

This work was supported by the National Natural Science Foundation of China (31770860, 21772164, 81572589, 81602560 and 21572187), and the Natural Science Foundation of Fujian Province (2018R1036-2, 2017J06020, 2019R1001-4, and 2019R1001-5).

■ ANCILLARY INFORMATION

Supporting Information.

The following files are available free of charge.

^{1}H and ^{13}C NMR spectra for all analogues and supplementary figures (PDF)

Molecular Formula Strings for **B1**-**B15** (CSV)

X-ray data for compound **B-12** (CIF)

Corresponding Author Information

Corresponding Authors

Yan-yan Zhan, E-mail: yyzhan@xmu.edu.cn, Tel: +86-592-2188223

Yandong Zhang, E-mail: ydzhang@xmu.edu.cn, Tel: +86-592-2181902

Tianhui Hu, E-mail: thu@xmu.edu.cn, Tel: +86-592-2188223

Author Contributions

T.H., Y.Z. and Y.-Y.Z. designed the experiments and wrote the manuscript. B.X., X.J, J.X., J.L., Y.T., L.Z., X.W., N.X., H.C., W.Z., H.Z., and X.H. carried out the experiments. The manuscript was written through the contributions of all authors. All authors have given approval to the final version of the manuscript.

Notes

The authors declare no competing financial interest.

■ REFERENCES

1. Gregorieff, A.; Clevers, H. Wnt Signaling in the Intestinal Epithelium: from Endoderm to Cancer. *Genes Dev.* **2005**, 19, 877–890.

2. Rustgi, A. K. Braf: A Driver of the Serrated Pathway in Colon Cancer. *Cancer Cell* **2013**, 24, 1–2.

3. Miller, K. D.; Siegel, R. L.; Lin, C. C.; Mariotto, A. B.; Kramer, J. L.; Rowland, J. H.; Stein, K. D.; Alteri, R.; Jemal, A. Cancer Treatment and Survivorship Statistics, 2016. *CA Cancer J. Clin.* **2016**, 66, 271–289.

4. De Lera, A. R.; Bourguet, W.; Altucci, L.; Gronemeyer, H. Design of Selective Nuclear Receptor Modulators: RAR and RXR as a Case Study. *Nat. Rev. Drug Discov.* **2007**, 6, 811–820.

5. Szanto, A.; Narkar, V.; Shen, Q.; Uray, I. P.; Davies, P. J.; Nagy, L. Retinoid X Receptors: X-Ploring Their (Patho)Physiological Functions. *Cell Death Differ.* **2004**, 11 Suppl 2, S126–S143.

6. Evans, R. M.; Mangelsdorf, D. J. Nuclear Receptors, RXR, and the Big Bang. *Cell* **2014**, 157, 255–266.

7. Yamazaki, K.; Shimizu, M.; Okuno, M.; Matsushima-Nishiwaki, R.; Kanemura, N.; Araki, H.; Tsurumi, H.; Kojima, S.; Weinstein, I. B.; Moriwaki, H. Synergistic Effects of RXRα and PPARγ Ligands to Inhibit Growth in Human Colon Cancer Cells—Phosphorylated RXRα Is a Critical Target for Colon Cancer Management. *Gut* **2007**, 56, 1557–1563.

8. Volate, S. R.; Muga, S. J.; Issa, A. Y.; Nitcheva, D.; Smith, T.; Wargovich, M. J. Epigenetic Modulation of the Retinoid X Receptor α by Green Tea in the Azoxymethane-*Apc*$^{min/+}$ Mouse Model of Intestinal Cancer. *Mol. Carcinog.* **2009**, 48, 920–933.

9. Tang, H.; Mirshahidi, S.; Senthil, M.; Kazanjian, K.; Chen, C. S.; Zhang, K. Down-Regulation of LXR/RXR Activation and Negative Acute Phase Response Pathways in Colon Adenocarcinoma Revealed by Proteomics and Bioinformatics Analysis. *Cancer Biomark.* **2014**, 14, 313–324.

10. Beildeck, M. E.; Gelmann, E. P.; Byers, S. W. Cross-Regulation of Signaling Pathways: An Example of Nuclear Hormone Receptors and the Canonical Wnt Pathway. *Exp. Cell Res.* **2010**, 316, 1763–1772.

11. Mulholland, D. J.; Dedhar, S.; Coetzee, G. A.; Nelson, C. C. Interaction of Nuclear Receptors with the Wnt/β-Catenin/Tcf Signaling Axis: Wnt You Like to Know? *Endocr. Rev.* **2005**, 26, 898–915.

12. Han, A.; Song, Z.; Tong, C.; Hu, D.; Bi, X.; Augenlicht, L. H.; Yang, W. Sulindac Suppresses β-Catenin Expression in Human Cancer Cells. *Eur. J. Pharmacol.* **2008**, 583, 26–31.

13. Zhang, F.; Meng, F.; Li, H.; Dong, Y.; Yang, W.; Han, A. Suppression of Retinoid X Receptor α and Aberrant β-Catenin Expression Significantly Associates with Progression of Colorectal Carcinoma. *Eur. J. Cancer* **2011**, 47, 2060–2067.

14. Xiao, J. H.; Ghosn, C.; Hinchman, C.; Forbes, C.; Wang, J.; Snider, N.; Cordrey, A.; Zhao, Y.; Chandraratna, R. A. Adenomatous Polyposis Coli (APC)-Independent Regulation of β-Catenin

Degradation via a Retinoid X Receptor-Mediated Pathway. *J. Biol. Chem.* **2003**, 278, 29954–29962.

15. Dillard, A. C.; Lane, M. A. Retinol Increases β-Catenin-RXRα Binding Leading to the Increased Proteasomal Degradation of β-Catenin and RXRα. *Nutr. Cancer* **2008**, 60, 97–108.

16. Dawson, M. I.; Zhang, X. K. Discovery and Design of Retinoic Acid Receptor and Retinoid X Receptor Class- and Subtype-Selective Synthetic Analogs of All-Trans-Retinoic Acid and 9-Cis-Retinoic Acid. *Curr. Med. Chem.* **2002**, 9, 623–637.

17. Perez, E.; Bourguet, W.; Gronemeyer, H.; de Lera, A. R. Modulation of RXR Function Through Ligand Design. *BBA-Mol. Cell Biol. L.* **2012**, 1821, 57–69.

18. Querfeld, C.; Nagelli, L. V.; Rosen, S. T.; Kuzel, T. M.; Guitart, J. Bexarotene in the Treatment of Cutaneous T-Cell Lymphoma. *Expert Opin. Pharmacother.* **2006**, 7, 907–915.

19. Chang, W.; Chen, L.; Hatch, G. M. Berberine As a Therapy for Type 2 Diabetes and Its Complications: From Mechanism of Action to Clinical Studies. *Biochem. Cell Biol.* **2015**, 93, 479–486.

20. Derosa, G.; Maffioli, P.; Cicero, A. F. Berberine on Metabolic and Cardiovascular Risk Factors: An Analysis from Preclinical Evidences to Clinical Trials. *Expert Opin. Biol. Ther.* **2012**, 12, 1113–1124.

21. Liu, D.; Meng, X.; Wu, D.; Qiu, Z.; Luo, H. A Natural Isoquinoline Alkaloid with Antitumor Activity: Studies of the Biological Activities of Berberine. *Front. Pharmacol.* **2019**, 10, 9.

22. Zhang, Z.; Zhang, H.; Li, B.; Meng, X.; Wang, J.; Zhang, Y.; Yao, S.; Ma, Q.; Jin, L.; Yang, J.; Wang, W.; Ning, G. Berberine Activates Thermogenesis in White and Brown Adipose Tissue. *Nat. Commun.* **2014**, 5, 5493.

23. Tillhon, M.; Guaman Ortiz, L. M.; Lombardi, P.; Scovassi, A. I. Berberine: New Perspectives for Old Remedies. *Biochem. Pharmacol.* **2012**, 84, 1260–1267.

24. Ortiz, L. M.; Lombardi, P.; Tillhon, M.; Scovassi, A. I. Berberine, an Epiphany Against Cancer. *Molecules* **2014**, 19, 12349–12367.

25. Wang, L.; Liu, L.; Shi, Y.; Cao, H.; Chaturvedi, R.; Calcutt, M. W.; Hu, T.; Ren, X.; Wilson, K. T.; Polk, D. B.; Yan, F. Berberine Induces Caspase-Independent Cell Death in Colon Tumor Cells through Activation of Apoptosis-Inducing Factor. *PLoS One* **2012**, 7, e36418.

26. Ruan, H.; Zhan, Y. Y.; Hou, J.; Xu, B.; Chen, B.; Tian, Y.; Wu, D.; Zhao, Y.; Zhang, Y.; Chen, X.; Mi, P.; Zhang, L.; Zhang, S.; Wang, X.; Cao, H.; Zhang, W.; Wang, H.; Li, H.; Su, Y.; Zhang, X. K.; Hu, T. Berberine Binds RXRα to Suppress β-Catenin Signaling in Colon Cancer Cells. *Oncogene* **2017**, 36, 6906–6918.

27. Rawat, D. S.; Thakur, B. K.; Semalty, M.; Semalty, A.; Badoni, P.; Rawat, M. S. Baicalein-Phospholipid Complex: A Novel Drug Delivery Technology for Phytotherapeutics. *Curr. Drug. Discov. Technol.* **2013**, 10, 224–232.

28. Oh, Y. J.; Choi, G.; Choy, Y. B.; Park, J. W.; Park, J. H.; Lee, H. J.; Yoon, Y. J.; Chang, H. C.; Choy, J. H. Aripiprazole-Montmorillonite: A New Organic-Inorganic Nanohybrid Material for Biomedical Applications. *Chem. Eur. J.* **2013**, 19, 4869–4875.

29. Park, K. D.; Lee, J. H.; Kim, S. H.; Kang, T. H.; Moon, J. S.; Kim, S. U. Synthesis of 13-(Substituted Benzyl) Berberine and Berberrubine Derivatives as Antifungal Agents. *Bioorg. Med. Chem. Lett.* **2006**, 16, 3913–3916.

30. Samosorn, S.; Tanwirat, B.; Muhamad, N.; Casadei, G.; Tomkiewicz, D.; Lewis, K.; Suksamrarn, A.; Prammananan, T.; Gornall, K. C.; Beck, J. L.; Bremner, J. B. Antibacterial Activity of Berberine-Nora Pump Inhibitor Hybrids with a Methylene Ether Linking Group. *Bioorg. Med. Chem.* **2009**, 17, 3866–3872.

31. Grycova, L.; Hulova, D.; Maier, L.; Standara, S.; Necas, M.; Lemiere, F.; Kares, R.; Dostal, J.; Marek, R. Covalent Bonding of Azoles to Quaternary Protoberberine Alkaloids. *Magn. Reson. Chem.* **2008**, 46, 1127–1134.

32. Zhang, H.; Wei, J.; Xue, R.; Wu, J. D.; Zhao, W.; Wang, Z. Z.; Wang, S. K.; Zhou, Z. X.; Song, D. Q.; Wang, Y. M.; Pan, H. N.; Kong, W. J.; Jiang, J. D. Berberine Lowers Blood Glucose in Type 2 Diabetes Mellitus Patients through Increasing Insulin Receptor Expression. *Metabolism* **2010**, 59, 285–292.

33. Cheng, Z.; Chen, A. F.; Wu, F.; Sheng, L.; Zhang, H. K.; Gu, M.; Li, Y. Y.; Zhang, L. N.; Hu, L. H.; Li, J. Y.; Li, J. 8,8-Dimethyldihydroberberine with Improved Bioavailability and Oral Efficacy on Obese and Diabetic Mouse Models. *Bioorg. Med. Chem.* **2010**, 18, 5915–5924.

34. Song, L.; Zhang, H. J.; Deng, A. J.; Li, J.; Li, X.; Li, Z. H.; Zhang, Z. H.; Wu, L. Q.; Wang, S. Q.; Qin, H. L. Syntheses and Structure-Activity Relationships on Antibacterial and Anti-Ulcerative Colitis Properties of Quaternary 13-Substituted Palmatines and 8-Oxo-13-Substituted Dihydropalmatines. *Bioorg. Med. Chem.* **2018**, 26, 2586–2598.

35. Jin, F.; Gao, D.; Wu, Q.; Liu, F.; Chen, Y.; Tan, C.; Jiang, Y. Exploration of N-(2-Aminoethyl)Piperidine-4-Carboxamide as a Potential Scaffold for Development of VEGFR-2, ERK-2 and Abl-1 Multikinase Inhibitor. *Bioorg. Med. Chem.* **2013**, 21, 5694–5706.

36. Bi, C. W.; Zhang, C. X.; Li, Y. B.; Zhao, W. L.; Shao, R. G.; Mei, L.; Song, D. Q. Synthesis and Structure-Activity Relationship of Cycloberberine as Anti-Cancer Agent. *Yao Xue Xue Bao* **2013**, 48, 1800–1806.

37. Gatland, A. E.; Pilgrim, B. S.; Procopiou, P. A.; Donohoe, T. J. Short and Efficient Syntheses of Protoberberine Alkaloids Using Palladium-Catalyzed Enolate Arylation. *Angew. Chem., Int. Ed.* **2014**, 53, 14555–14558.

38. Buck, J. S.; Davis, R. M. Pictet and Gams' Berberine Synthesis. *J. Am. Chem. Soc.* **1930**, 52, 660–664.

39. Moulis, C.; Gleye, J.; Stanislas, E. Alcaloïdes de l' Isopyrum Thalictroïdes—Bases Quaternaires des Feuilles—Isolement et Identification de Quatre Pseudoprotoberberines. *Phytochemistry* **1977**, 16, 1283–1287.

40. Sebe, E.; Abe, S.; Murase, N.; Shibata, Y. Supplementary Observations on the Chemistry of the Alkaloids of Berberine Series. II. The Ultraviolet Absorption Spectra of Berberines and Related Compounds. *J. Chin. Chem. Soc.* **1967**, 14, 135–160.

41. Murayama, Y.; Shinozaki, K. On the Alkaloids of Coptis Root. *Yakugaku Zasshi* **1926**, 1926, 299–302.

42. Yang, P.; Song, D.-Q.; Li, Y.-H.; Kong, W.-J.; Wang, Y.-X.; Gao, L.-M.; Liu, S.-Y.; Cao, R.-Q.; Jiang, J.-D. Synthesis and Structure–Activity Relationships of Berberine Analogues as a Novel Class of Low-Density-Lipoprotein Receptor Up-Regulators. *Bioorg. Med. Chem. Lett.* **2008**, 18, 4675–4677.

43. Wang, W.; Liu, H.; Wang, S.; Hao, X.; Li, L. A Diterpenoid Derivative 15-Oxospiramilactone Inhibits Wnt/β-Catenin Signaling and Colon Cancer Cell Tumorigenesis. *Cell Res.* **2011**, 21, 730–740.

44. Paruthiyil, S.; Parmar, H.; Kerekatte, V.; Cunha, G. R.; Firestone, G. L.; Leitman, D. C. Estrogen Receptor B Inhibits Human Breast Cancer Cell Proliferation and Tumor Formation by Causing a G2 Cell Cycle Arrest. *Cancer Res.* **2004**, 64, 423–428.

45. Lefebvre, P.; Benomar, Y.; Staels, B. Retinoid X Receptors: Common Heterodimerization Partners with Distinct Functions. *Trends Endocrinol. Metab.* **2010,** 21, 676–683.

46. Su, Y.; Zeng, Z.; Chen, Z.; Xu, D.; Zhang, W.; Zhang, X. K. Recent Progress in the Design and Discovery of RXR Modulators Targeting Alternate Binding Sites of the Receptor. *Curr. Top. Med. Chem.* **2017**, 17, 663–675.

47. Rochette-Egly, C. Retinoic Acid Signaling and Mouse Embryonic Stem Cell Differentiation: Cross Talk Between Genomic and Non-Genomic Effects of RA. *BBA-Mol. Cell Biol. L.* **2015**, 1851, 66–75.

48. Gilardi, F.; Desvergne, B. RXRs: Collegial Partners. *In Biochemistry of Retinoic Acid Receptors I: Structure, Activation, and Function at the Molecular Level,* Asson-Batres, M. A.; Rochette-Egly, C., Eds. Springer 2014; Vol. 70, pp 75–102.

49. Egea, P. F.; Mitschler, A.; Rochel, N.; Ruff, M.; Chambon, P.; Moras, D. Crystal Structure of the Human RXRα Ligand-Binding Domain Bound to Its Natural Ligand: 9-Cis Retinoic Acid. *EMBO J.* **2000**, 19, 2592–2601.

50. Burnett, A. K.; Russell, N. H.; Hills, R. K.; Bowen, D.; Kell, J.; Knapper, S.; Morgan, Y. G.; Lok, J.; Grech, A.; Jones, G.; Khwaja, A.; Friis, L.; McMullin, M. F.; Hunter, A.; Clark, R. E.; Grimwade, D.; Group, U. K. N. C. R. I. A. M. L. W. Arsenic Trioxide and All-Trans Retinoic Acid Treatment for Acute Promyelocytic Leukaemia in All Risk Groups (AML17): Results of a Randomised, Controlled, Phase 3 Trial. *Lancet Oncol.* **2015**, 16, 1295–1305.

51. Zhou, S.; Tong, R. A General, Concise Strategy that Enables Collective Total Syntheses of over 50 Protoberberine and Five Aporhoeadane Alkaloids within Four to Eight Steps. *Chem. Eur. J.* **2016**, 22, 7084–7089.

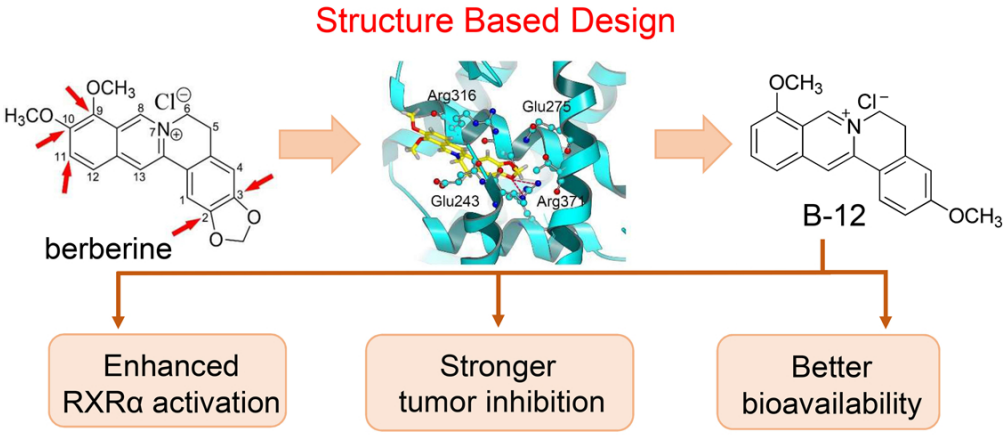

Table of Content Graphic

95x42mm (300 x 300 DPI)